AD-A070 140 SEDCO SYSTEMS INC MELVILLE N Y F/G 9/1
BROADBAND MAGIC TEE HYBRID.(U)
JUN 77 C H WU, T R DEBSKI N00173-76-C-0335
UNCLASSIFIED 3098-FTR NL

| OF |
AD A070140

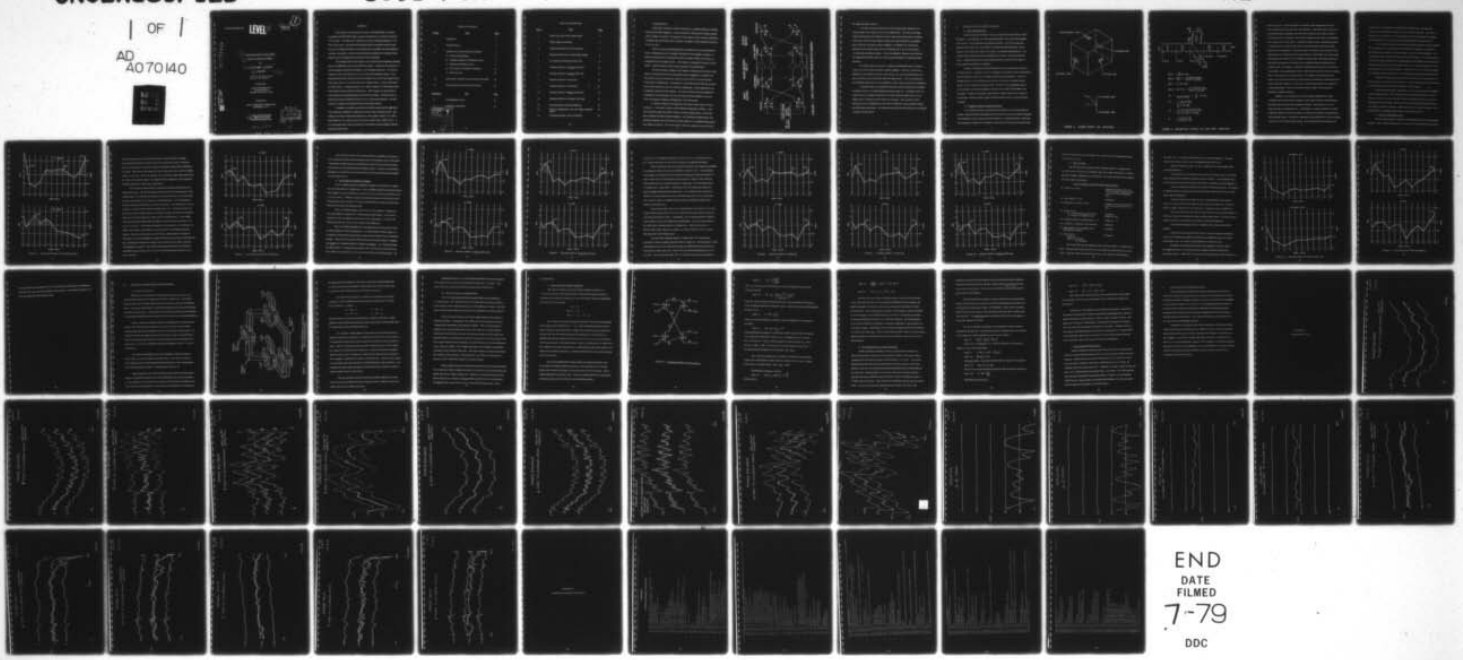

END
DATE FILMED
7-79
DDC

SEDCO SYSTEMS INC.

LEVEL II

(14) 3098-FTR
June 1977

(1)

AD A070140

(6) BROADBAND MAGIC TEE HYBRID.

(7) FINAL TECHNICAL REPORT.

BY

(10) C. H. WU and T. R. DEBSKI

(11) JUNE 1977 (12) 65 p.

APPROVED FOR PUBLIC RELEASE
DISTRIBUTION UNLIMITED

Prepared by:

SEDCO SYSTEMS INC.
65 Marcus Drive
Melville, New York 11746

Prepared for:

NAVAL RESEARCH LABORATORY
Washington, D. C.

(15) Under Contract Number
N00173-76-C-0335
Item 0002 Sequence A002

400 588 LB

ABSTRACT

This program was conducted to develop a Broadband Magic Tee Hybrid compatible with WRD750D24 ridge waveguide operating over a frequency band from 7.5 to 18 GHz. The hybrid tee is designed for a power handling capability of 1 Kw CW or 10 Kw peak. The device will find application in waveguide matrices which are used to combine the output of several high power traveling wave tube amplifiers operating in parallel, as well as in the fabrication of high power waveguide switch networks and as monopulse beam forming devices in antennas.

The principal effort of the program was directed toward impedance matching the sum and difference ports of the hybrid tee junction. Laboratory brassboards, as well as aluminum production prototypes, were fabricated and tested. The desired maximum VSWR of the device was 1.5:1 over the entire frequency range. It was demonstrated that this VSWR level could be obtained over most of the frequency band with a peak value of 1.7:1 at the edges of the frequency band. As part of the hybrid tee design effort, a computer program was written to analyze the VSWR performance of the hybrid in terms of physical dimensions. This program was found useful in determining the first approximation for the hybrid tee design. Empirical tests on laboratory brassboard hybrids provided a closer second approximation. The final design was completed in aluminum production prototype models.

In addition, an analysis was performed which demonstrated the application of the hybrid tee junctions to a high power four port ridge waveguide matrix. The analysis led to the conclusion that hybrid tees, with a typical VSWR of 1.5:1 and a peak VSWR of 1.7:1, could be used to construct a matrix with a VSWR of 2.2:1. It is recommended that a four-port matrix be constructed to experimentally verify the projected performance.

TABLE OF CONTENTS

Section	Title	Page
	ABSTRACT	i
I	INTRODUCTION	1
II	HYBRID TEE DEVELOPMENT PROGRAM	4
	A. General Considerations	4
	B. Computer Analysis of Equivalent Circuit	4
	C. Laboratory Brassboard Tests	8
	D. Test results for Aluminum Prototypes	12
	E. Final Test Data	19
III	ANALYSIS OF HYBRID APPLICATION TO MATRIX	24
IV	CONCLUSIONS AND RECOMMENDATIONS	34

Appendices	Title	Page
A	PERFORMANCE DATA	A1
B	COMPUTER PROGRAM	B1

LIST OF ILLUSTRATIONS

Figure	Title	Page
1	High-Power Four-Throw Switch Matrix	2
2	Hybrid Magic Tee Junction	5
3	Equivalent Circuit of Sum Port Junction	6
4	Measured VSWR Data For Theoretical Design	9
5	Best Observed Brassboard VSWR Data	11
6	Aluminum Hybrid 1-2 Brazed VSWR Data	13
7	Aluminum Hybrid 3-4 Brazed VSWR Data	14
8	Aluminum Hybrid 5-6 VSWR Data	16
9	Aluminum Hybrid 7-8 VSWR Data	17
10	Aluminum Hybrid 7-8 Brazed VSWR Data	18
11	Aluminum Hybrid 5-6 Colinear VSWR Data	21
12	Final Brassboard VSWR Data (Step 30)	22
13	Physical Configuration, Four Port Ridge Waveguide Matrix	25
14	Connections Within a Four-Port Matrix	29

I INTRODUCTION

Many future microwave systems will require a combined high power handling and broad bandwidth capability. A key component in a large number of these systems will be a Magic Tee Hybrid. The purpose of this program was to develop a hybrid tee, compatible with WRD750D24 ridge waveguide, operating over the frequency band from 7.5 to 18.0 GHz.

Since one of the principal applications of hybrid tee is in the construction of power combining networks for multiple traveling wave tube amplifier systems, an analysis was performed to determine the effects of hybrid VSWR on the VSWR of a complete four port waveguide matrix. That analysis is presented in Section 3 of this report. A brief summary of basic matrix operation is presented below.

The basic technique employed in the design of a high power four throw switch matrix is the insertion of the four traveling wavetube amplifiers in a section of the RF network where the only function required from the TWT's is to provide phase matched power amplification. The properties of the network insure that the combined power will be delivered to any one of the four output ports. These output ports may be typically connected to four antennas. The system will then have the capability of switching the combined power of the four traveling wavetube amplifiers to any one of the four antennas in typical switching times of 25 nanoseconds.

A schematic diagram of the high power four throw switch matrix is shown in Figure 1. The network consists of four principal components as follows: a low-power four throw high-speed diode switch, a low-power input matrix, a set of four phase-matched traveling wavetube amplifiers, and a high-power output matrix. The principal component of both the input and output matrices is a broadband high performance magic tee network. It is seen in Figure 1 that four magic tees are used in both

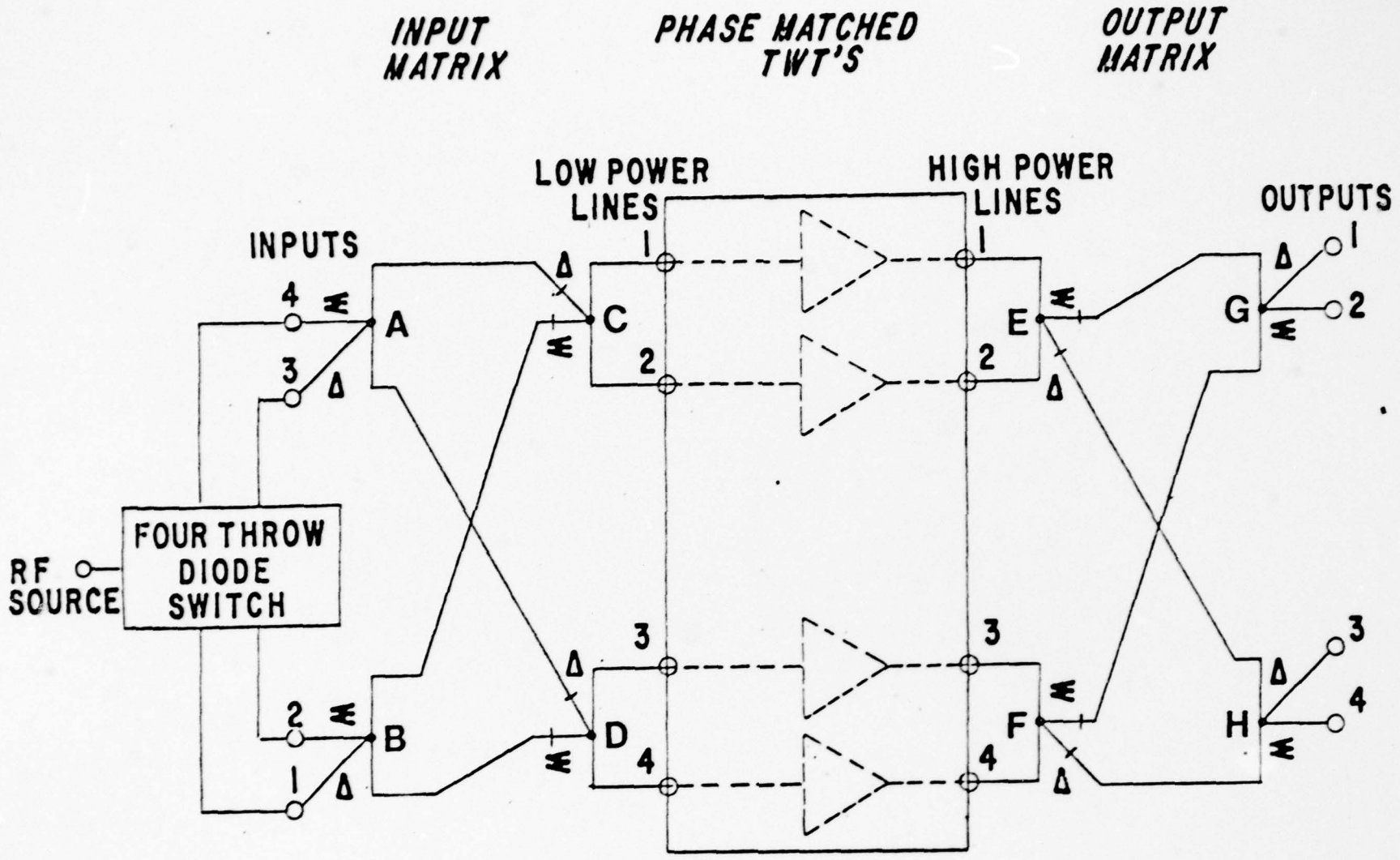

FIGURE 1 HIGH-POWER FOUR-THROW SWITCH MATRIX

the output and input matrices.

To a large extent the performance of the overall system depends on the characteristics of the magic tee used in the output matrix. The loss in the output matrix will deteriorate the efficiency of the overall system and provide a reduction in the power delivered at the output terminals from that available by summing the power of the four traveling wavetube amplifiers. In addition, the VSWR at the input ports of the output matrix must be sufficiently low so as not to deteriorate or damage the traveling wavetubes. Phase and amplitude coherence must obviously be maintained in both the magic tees and the interconnecting RF transmission lines and bends.

The input matrix does not have a rigid loss specification since it is located at the low level side of the traveling wavetube amplifiers. However, it does have a rigid phase and amplitude coherence requirement. It is recommended that the same type of network be used for both the input and output matrix. This is considered the most efficient solution from a cost standpoint as well as from a performance standpoint.

As indicated above, the principal component used in the high power broadband waveguide matrix is a broadband high performance magic tee. A guideline which was adopted for the tee design was that the low VSWR be obtained without the use of any tuning screws or dielectric blocks inside the waveguide. This provides a device which has very low dissipative loss and which is suitable for mass production without any final tuning requirement. The design and development of the hybrid tee is described in Section 2 of this report.

II HYBRID TEE DEVELOPMENT PROGRAM

A. General Considerations

A hybrid magic tee junction is a passive reciprocal four-port device, shown in Figure 2. Consequently, the main engineering problem associated with designing such a device is one of impedance-matching the junction. Once the sum port and difference port of the device are matched, the other desirable properties, such as colinear arm isolation and colinear arm match, are attained automatically as a consequence of the scattering matrix relationships in a lossless, reciprocal four port device. Isolation between the sum and difference ports is inherent in the device as long as physical symmetry is maintained.

Methods of matching the junction include the use of transformers, stubs and reactive obstacles. In practice, the exact technique used depends on other considerations such as dissipated losses, power handling capacity and reproducibility. In terms of dissipated losses, it is desirable to avoid the use of dielectric materials, bonding agents or screws inside the waveguide cavity. In terms of power handling capacity, it is desirable to avoid sharp capacitive obstacles or low height constrictions in the waveguide. Finally, the matching design should be readily reproduced by casting or numerically controlled milling machine techniques without need for custom trimming or tuning.

B. Computer Analysis of Equivalent Circuit

In an attempt to study and determine the feasibility of a wide-band magic tee design, a transmission line equivalent circuit was evolved as part of a previous program. This equivalent circuit is shown at the top of Figure 3. Transmission line 1 represents a line running essentially from the flange of the sum port to the actual sum port junction

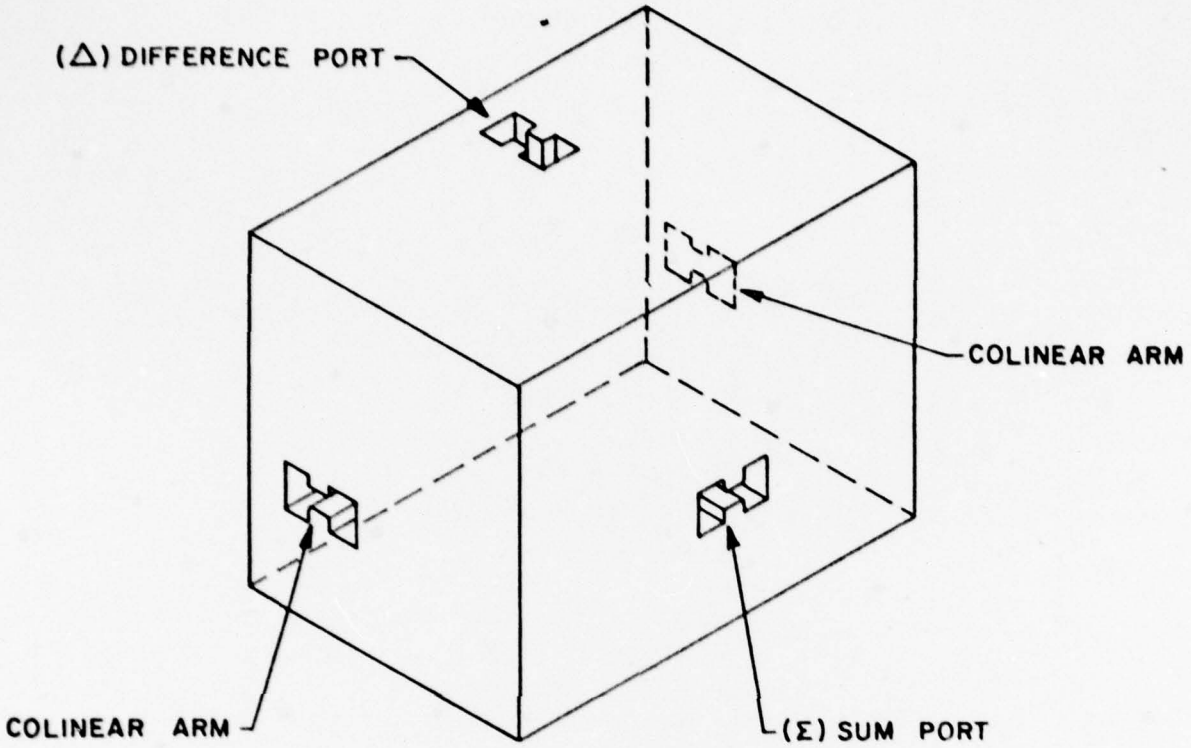

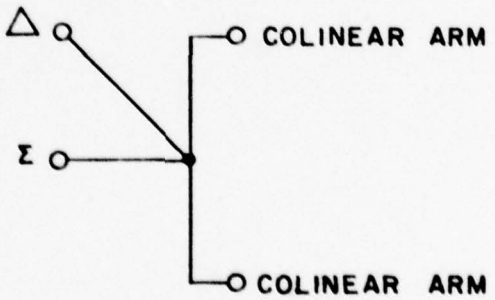

FIGURE 2 HYBRID MAGIC TEE JUNCTION

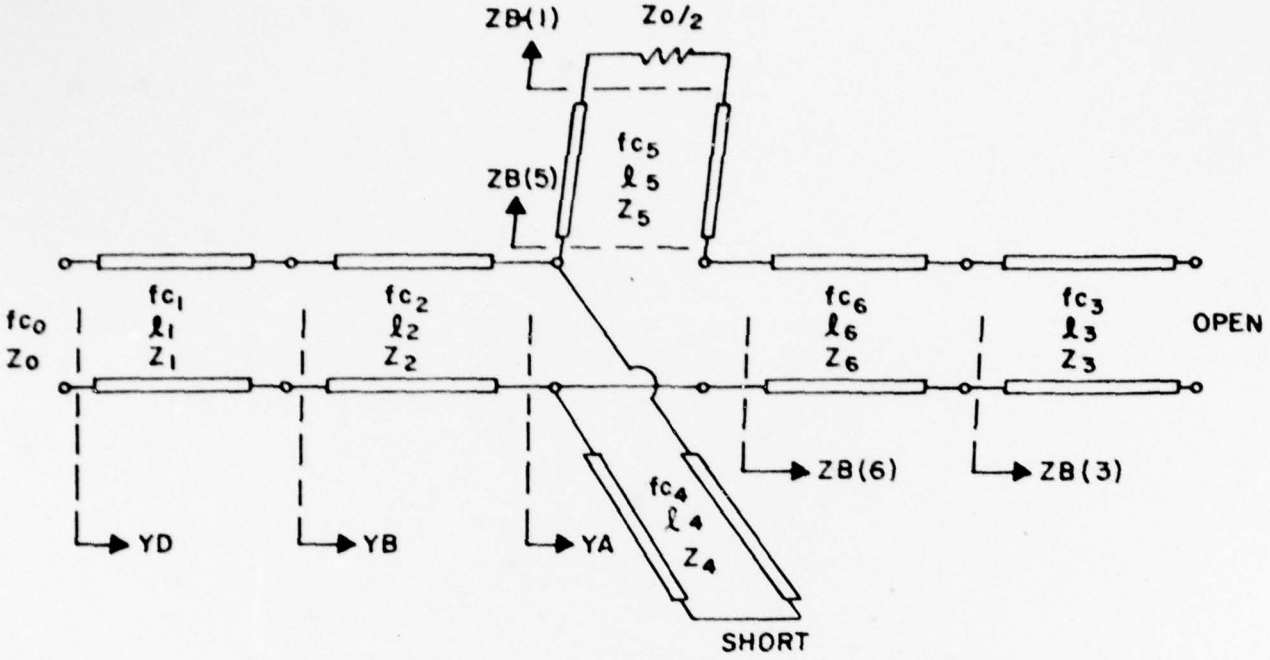

$$ZB(3) = j\left(\frac{Z3}{Z6}\right) \text{Cot } \beta\ell_3$$

$$ZB(6) = \left(\frac{Z6}{Z3}\right) / \left(\frac{1 + j\, ZB(3) \tan \beta\ell_6}{ZB(3) + j \tan \beta\ell_6}\right)$$

$$ZB(1) = (Z1/(2 \times Z5))$$

$$ZB(5) = (Z5/Z3) / \left(\frac{1 + j\, ZB(1) \tan \beta\ell_5}{ZB(1) + j \tan \beta\ell_5}\right)$$

$$YA = \frac{1}{ZB(5) + ZB(6)} - j\frac{Z_2}{Z_4} \text{ Cot } \beta\ell_4$$

$$YB = \frac{1 + j\frac{1}{YA} \tan \beta\ell_2}{\frac{1}{YA} + j \tan \beta\ell_2}$$

$$YD = \frac{1 + j\,(Z_2/(Z_1\, YB)) \tan \beta\ell_1}{(Z_2/(Z_1\, YB)) + j \tan \beta\ell_1}$$

$$\rho = \frac{1 - (Z_0/Z_1)\, YD}{1 + (Z_0/Z_1)\, YD}$$

FIGURE 3 EQUIVALENT CIRCUIT OF SUM PORT JUNCTION

at the cavity wall. Transmission line 2 represents a line running from the cavity wall to approximately the center line of the junction. Transmission line 4 represents a transmission path continuing to the blind wall at the back of the magic tee device. Transmission line 5 represents a pair of lines running from the center of the junction to the colinear arms of the hybrid. The pair of colinear arms, connected in parallel, is represented by a resistor whose value is equal to one-half of the characteristic impedance of the ridgeguide. Transmission line 6 represents a line formed by a thin septum placed in the difference port of the hybrid tee. Specifically, line 6 represents that portion of the septum which is within the junction cavity, and transmission line 3 represents that portion of the septum which is contained within the difference port waveguide run. The septum is excited in a symmetrical fashion by the sum port and, consequently, waves propagating on line 3 cannot proceed beyond the end of the septum, which is characterized as an open circuit. The equations in the lower portion of Figure 3 are used to calculate the sum port reflection coefficient at reference plane YD (shown in the top of Figure 3). Each of the six transmission lines is characterized by three parameters. These are cut-off frequency, length, and characteristic impedance at infinite frequency.

Initially, it was attempted to solve the equations graphically by using a combination of transmission line rotations, Carter chart impedance transformations, and Smith chart reactance and susceptance additions. This proved to be a very tedious and time consuming process. Consequently, a computer routine was written to find the solution to the above equations as a function of frequency and transmission line parameter values. The data was calculated at 23 frequencies (0.5 GHz increments) over the 7.0 to 18.0 GHz frequency band. The transmission line parameters were

adjusted using a combination of calculated cut-off frequencies, characteristic impedances, actual physical lengths, and some heuristic reasoning. The choice of parameters was reiterated on a semi-empirical basis until reasonable correlation between laboratory-measured data and computed analytical data was achieved.

As a result of the analysis performed on the prior program, it was concluded that a waveguide cross-section similar to WRD500D36 ridgeguide was required in the junction region of the tee in order to obtain a 7.5 to 18.0 GHz bandwidth. This conclusion led to the initial brassboard design for this program. The design is based on the use of standard WRD750D24 waveguide flanges with multiple-section step-down transformers leading to the actual junction region. The cut-off frequency is 6.3 GHz at the flanges and 4.9 GHz at the junction. This allows the use of a much less dispersive matching network and provides a correspondingly improved operating bandwidth.

During the beginning of this program, the solution for the input impedance of the circuit shown in Figure 3 was programmed for the Hewlett Packard 9825 calculator. A copy of that program is included as Appendix B of this report.

Based upon this program, dimensions were chosen for the initial brassboard model matching network. The resulting VSWR of the theoretical design is shown in Figure 4. It can be seen from the figure that the equivalent circuit was very useful in obtaining a first cut design. However, since the analytical model did not include such effects as junction reactances, higher order modes or contact resistance, it was of limited value in obtaining further improvements in performance.

C. Laboratory Brassboard Tests

Two brassboard magic tee hybrids were fabricated as part of the development program. Brass, rather than aluminum, was chosen so that additional metal could be

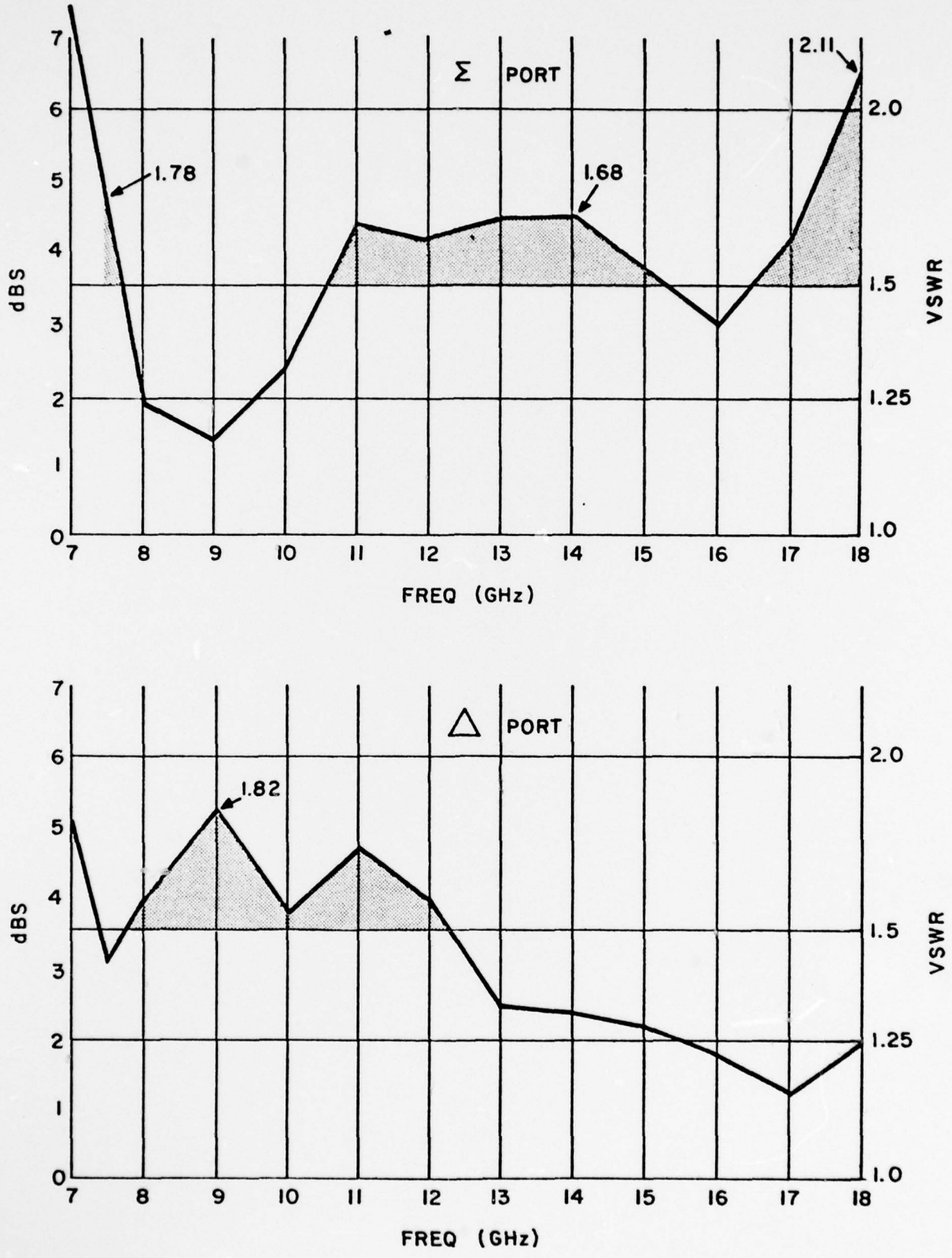

FIGURE 4 - Measured VSWR Data For Theoretical Design

soldered in place when ever design modifications required this type of change. Starting with the theoretical design discussed in the previous section, an iterative process of microwave measurement, engineering analysis and test part modification was begun. Many dimensional changes (29 major Steps) were made, and the resulting VSWR was observed. Most of the changes were made in the metal septum which forms the center of the junction region. One change involved modification of the impedance matching transformers in the arms of the hybrid.

These iterative design changes resulted in the gradual improvement of the VSWR performance. The brassboard program also led to the conclusion that a VSWR of better than 1.5:1 could only be achieved over 80 percent of the 7.5 to 18 GHz band, and that a peak VSWR of 1.7:1 would occur at the band edges. The last significant improvement in brassboard data was observed in Step 29. This VSWR data, as shown in Figure 5, indicated a peak VSWR of slightly under 1.7:1. Subsequent to this test, the model was disassembled and then reassembled, using solder instead of conductive adhesive at the joints between the septum and the waveguide blocks. The resulting data (called Step 29B) indicated that the difference port VSWR increased from 1.68:1 to 1.97:1 at 18 GHz. Two possible explanations for the change are: (1) different conductive characteristics of conductive cement and solder or (2) slight dimensional changes. Since the second cause was more likely, a slight change to the Step 29B dimensions was made by shifting the septum 0.002 inches upward towards the difference port, extending the difference port ridges 0.005 down toward the septum, and then resoldering the assembly. This resulted in the Step 29C data where the difference port VSWR decreased from 1.97:1 to 1.44:1 at 18 GHz but increased from 1.66:1 to 1.84:1 at 9 GHz.

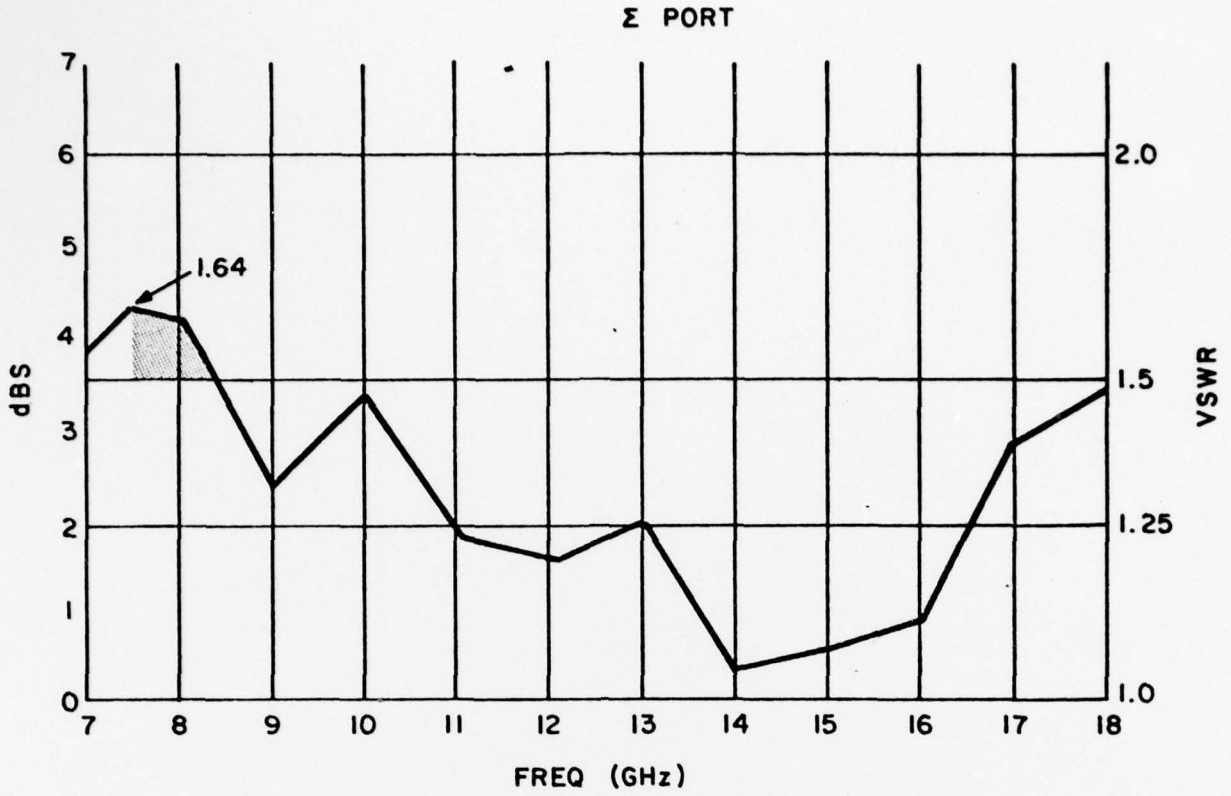

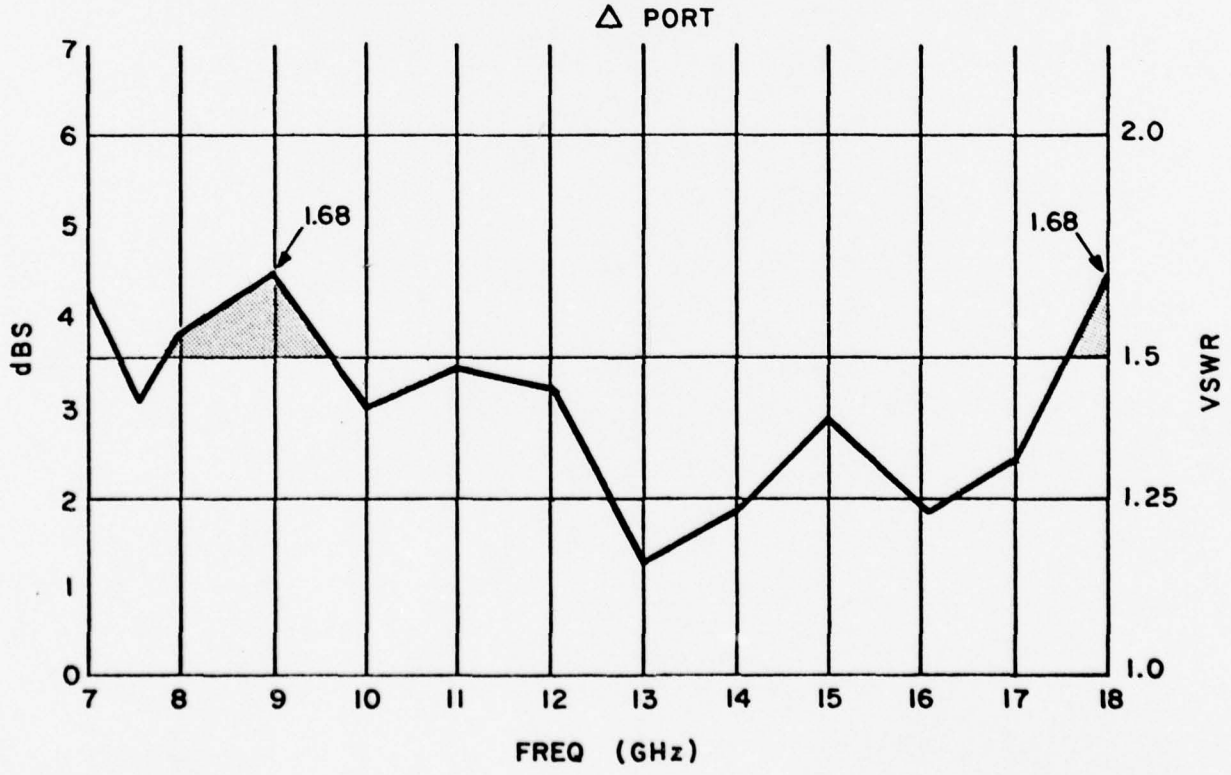

FIGURE 5 - Best Observed Brassboard VSWR Data

Based on these results, it was concluded that the variability in the data was due to extremely sensitive dimensional tolerances in the junction region of the hybrid. Consequently, further brassboard modifications would not yield an improved choice of dimensions for the initial aluminum prototype hybrids. Therefore, two aluminum prototypes were built based on the best brassboard dimensional information available from all steps up to 29.

D. Test Results for Aluminum Prototypes

The two original aluminum prototypes, designated "Alum Hybrid 1-2 Septum one" and "Alum Hybrid 3-4 Septum one", were essentially identical in their performance. They exhibited a sum port VSWR of 1.88:1 and 1.95:1 at 7.5 GHz but the VSWR was only 1.10:1 at 18 GHz. A change was made in the septum design to favor the low end of the frequency band in the sum port. It was also expected that this change would favor the high end of the band in the difference port.

The two modified prototypes, referred to as "Alum Hybrid 1-2 Septum two" and "Alum Hybrid 3-4 Septum two", yielded improved performance. The sum port VSWR at 7.5 GHz was improved to 1.80:1 and 1.78:1 respectively. At 18 GHz, the VSWR increased from 1.10:1 to 1.35:1 which is still within spec.

These two modified prototypes were then dip-brazed to determine the extent of VSWR change due to the brazing process. A certain amount of VSWR change is to be expected, primarily due to dimensional changes and secondarily due to conductivity changes. Figures 6 and 7 show the VSWR data for the "Aluminum Hybrid 1-2 Septum two Brazed" and "Aluminum Hybrid 3-4 Septum two Brazed". As a result of brazing, the VSWR of the "1-2" Hybrid increased from 1.80:1 to 1.84:1 at 7.5 GHz in the sum port, while it decreased from 1.60:1 to 1.53:1 at 8.0 GHz in the difference port. The

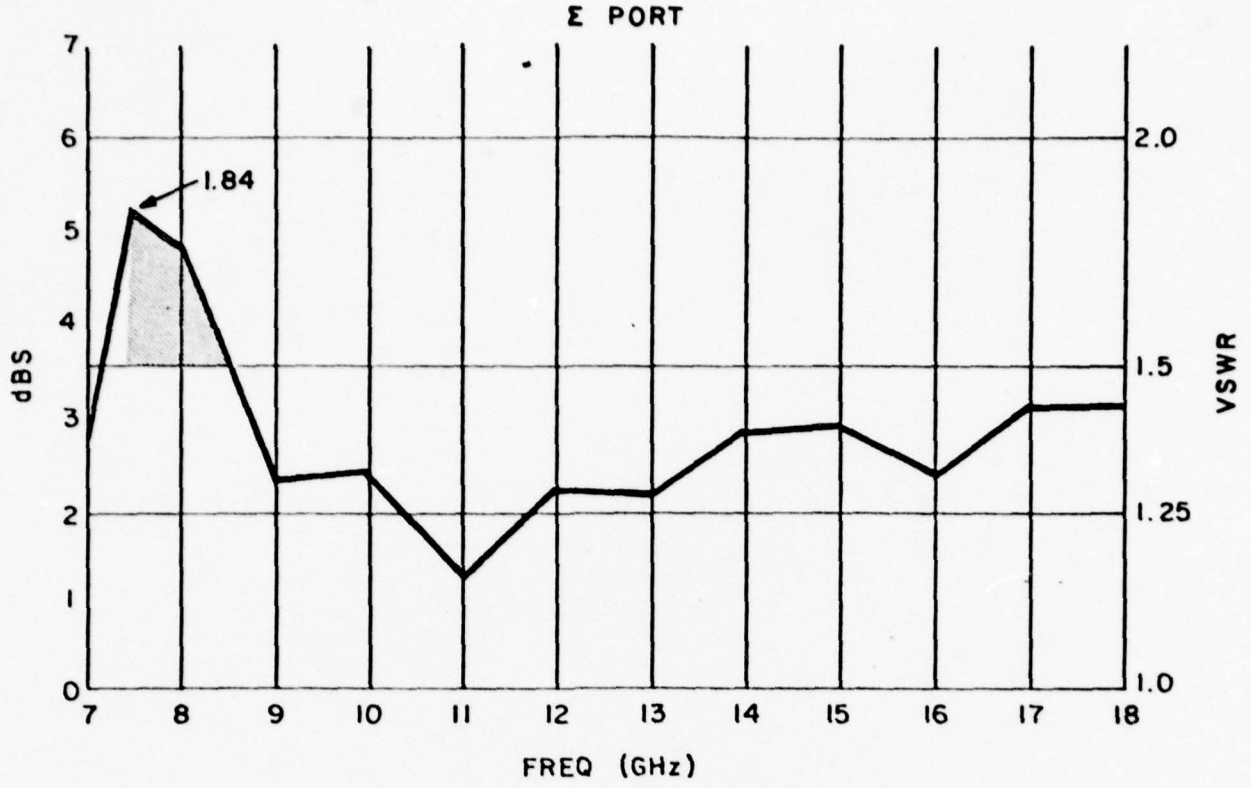

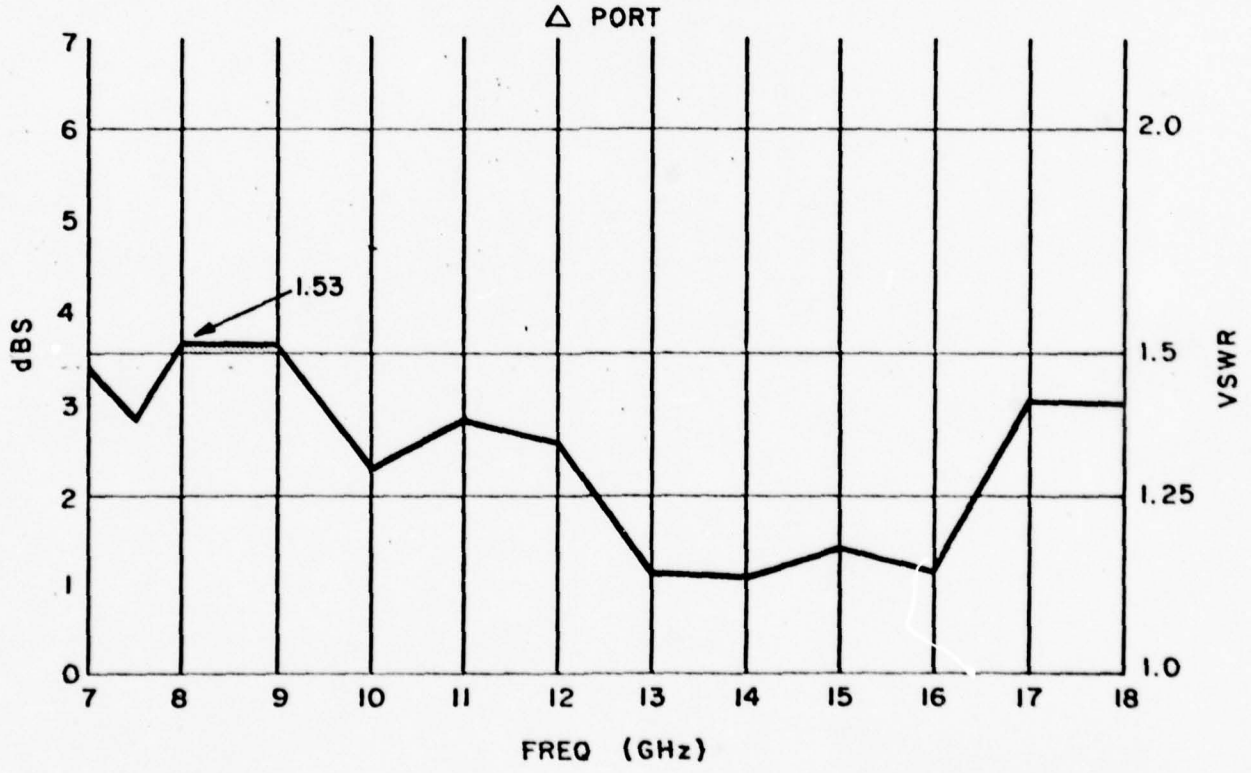

FIGURE 6 - Aluminum Hybrid 1-2 Brazed VSWR Data

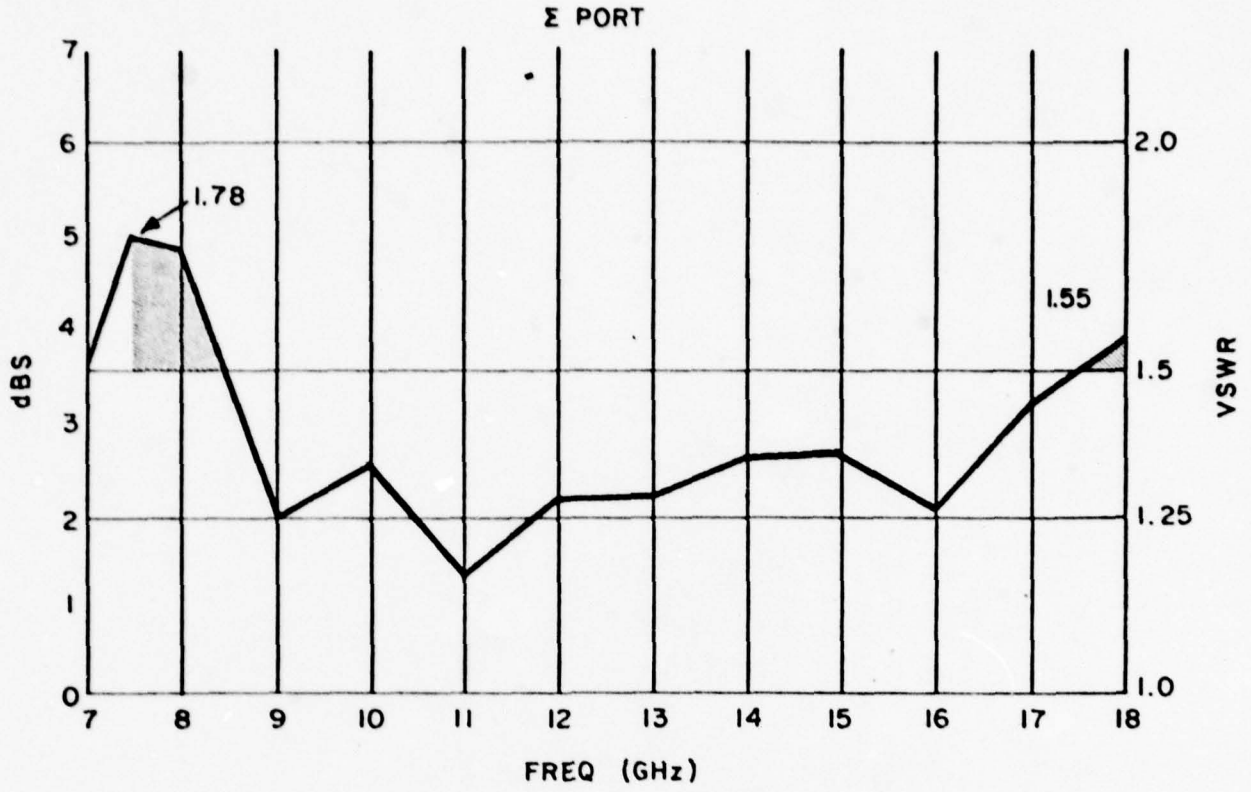

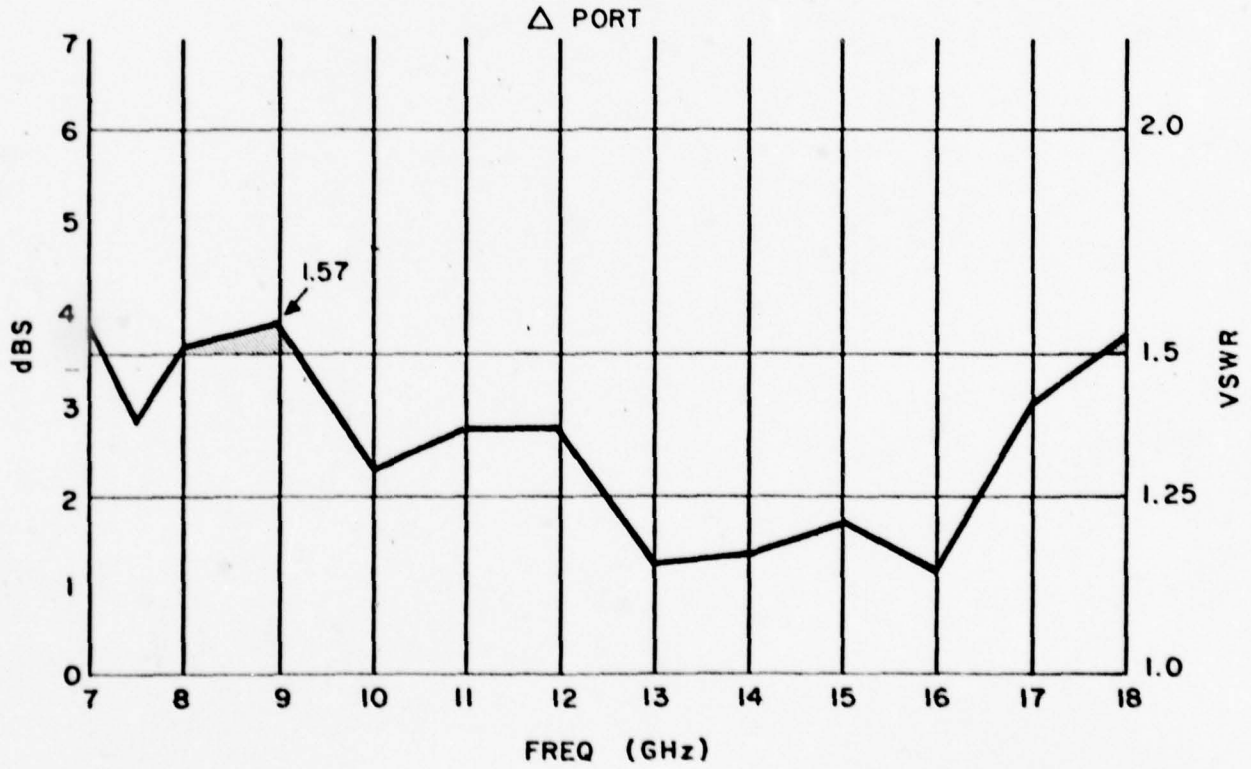

FIGURE 7 - Aluminum Hybrid 3-4 Brazed VSWR Data

VSWR of the "3-4" Hybrid increased from 1.33:1 to 1.55:1 at 18.0 GHz in the sum port, while performance over the rest of the band was essentially unchanged.

Based on the above data, it was decided to build two more aluminum prototypes in an attempt to improve the sum port VSWR at 7.5 GHz to 1.70:1. The dimensions of the septum were changed to trade-off midband and high end VSWR performance to achieve improved low end performance in the sum port. Figures 8 and 9 show the VSWR performance for "Aluminum Hybrid 5-6 Septum four" and "Aluminum Hybrid 7-8 Septum three" respectively. In the former case, the dimensional change was pursued slightly further than in the latter case. As a result it can be seen that the VSWR at 7.5 GHz is improved to 1.64:1 in the first case and to 1.74:1 in the second case. However, there is a slightly greater sacrifice in midband and high end performance in the first case.

Based upon the above data, it was concluded that a peak VSWR of 1.75:1 with a typical VSWR of better than 1.55:1 over 80 percent of the band could be expected in a dip-brazed production version. Consequently, it was requested that this relatively minor change be made to the performance specification. As can be seen in Figure 8, the VSWR of the "Aluminum Hybrid 5-6 Septum four", which was delivered as line item 0001 of this contract, is actually 1.64:1 peak and under 1.53:1 over more than 80 percent of the frequency band.

It is noted that "Aluminum Hybrid 7-8 Septum three" was subsequently dip-brazed, with the resulting VSWR data shown in Figure 10. Comparing these results with Figure 9, it can be seen that after brazing, the midband performance improved from 1.55:1 to better than 1.50:1, while the low end VSWR deteriorated from 1.74:1 to 1.84:1. These results infer that, if the "5-6" unit were brazed, its midband per-

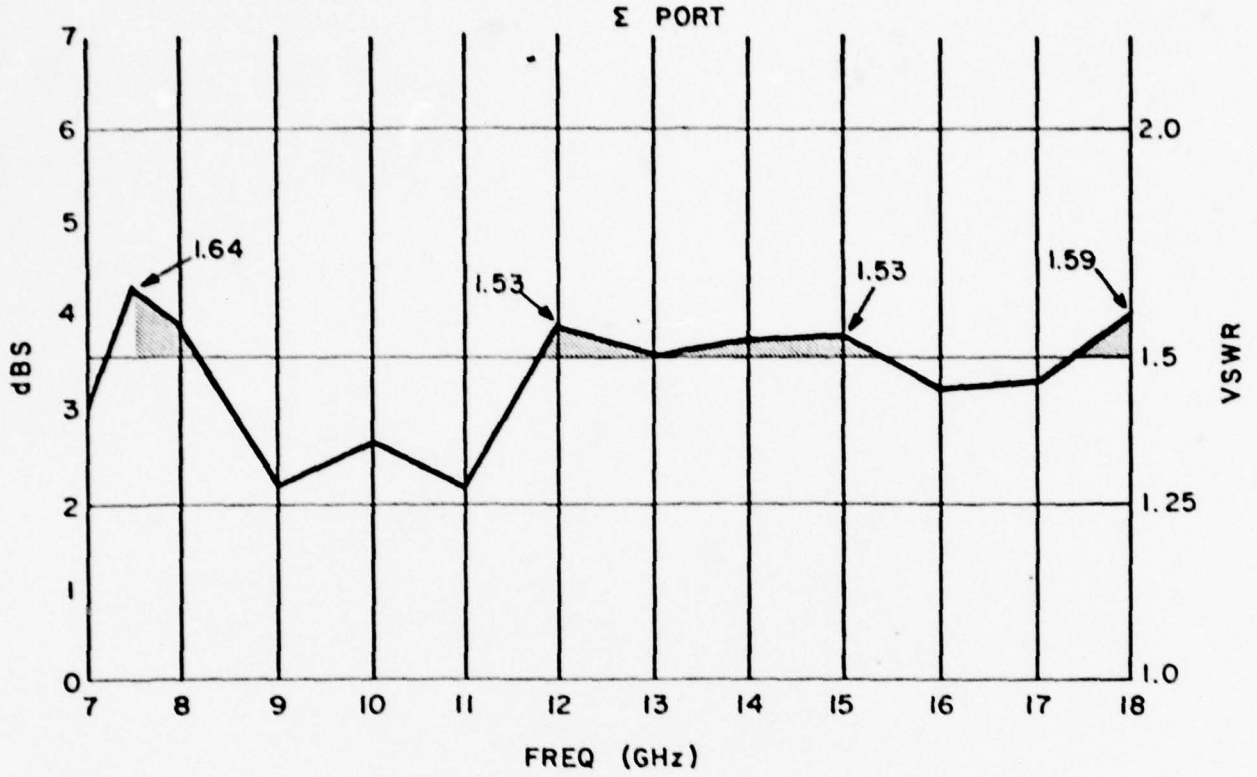

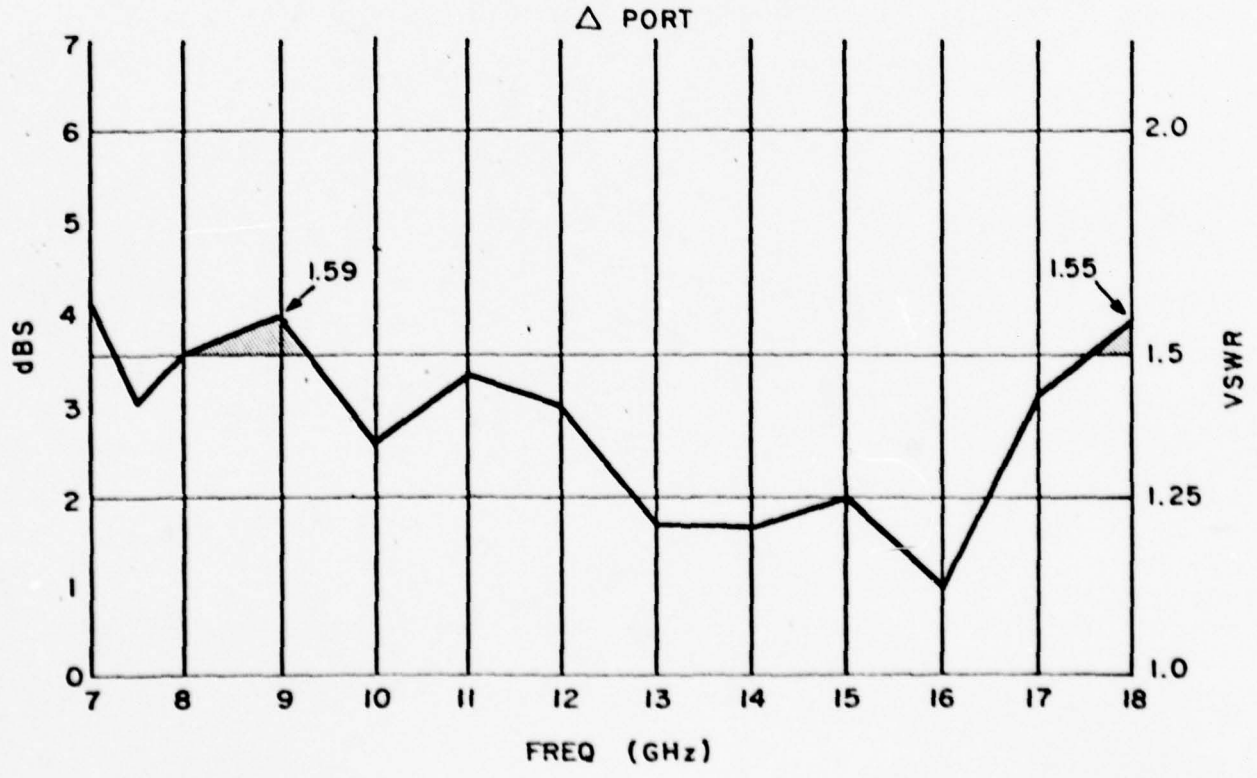

FIGURE 8 - Aluminum Hybrid 5-6 VSWR Data

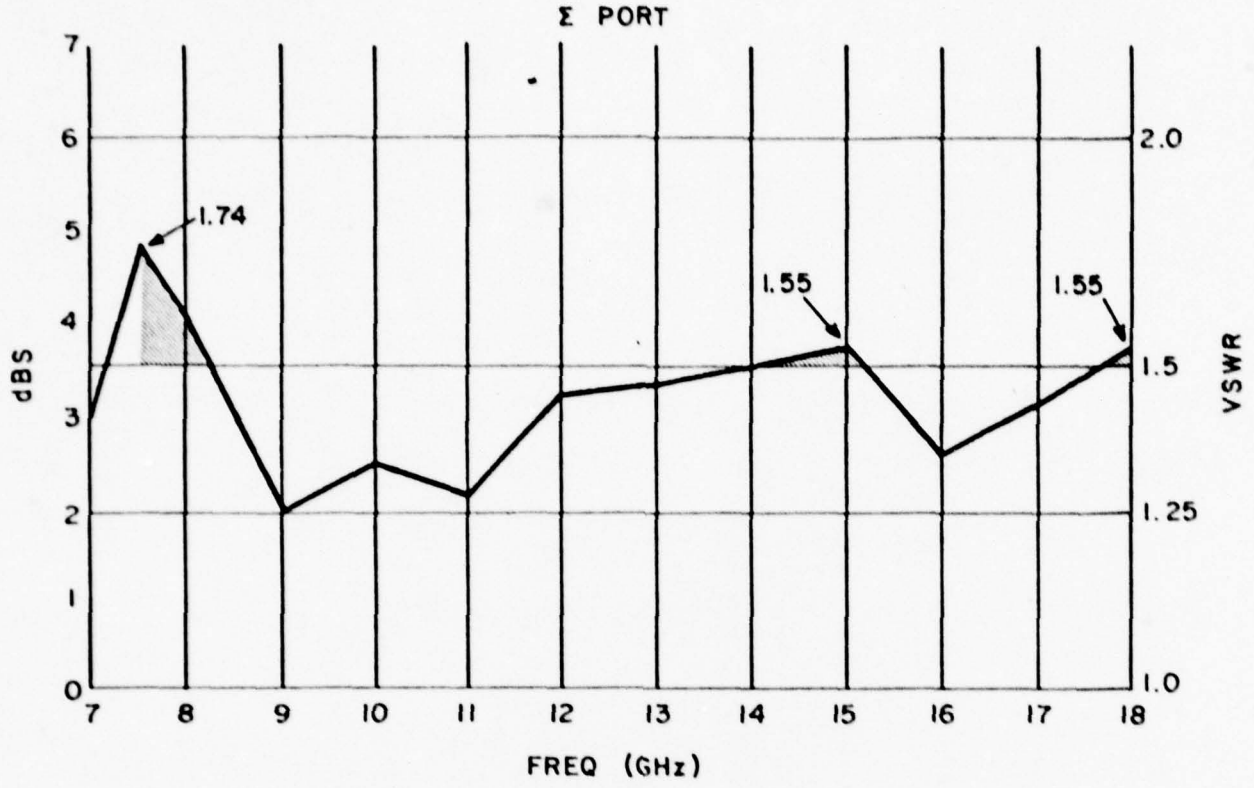

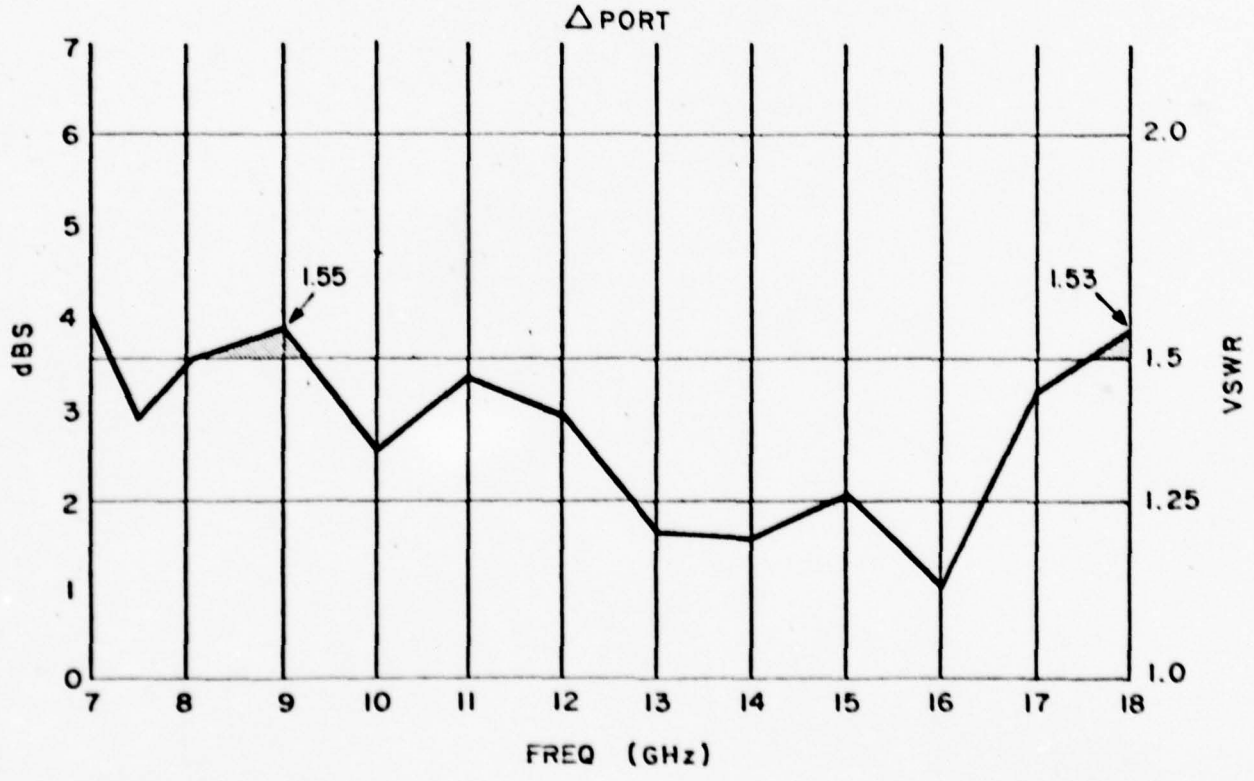

FIGURE 9 - Aluminum Hybrid 7-8 VSWR Data

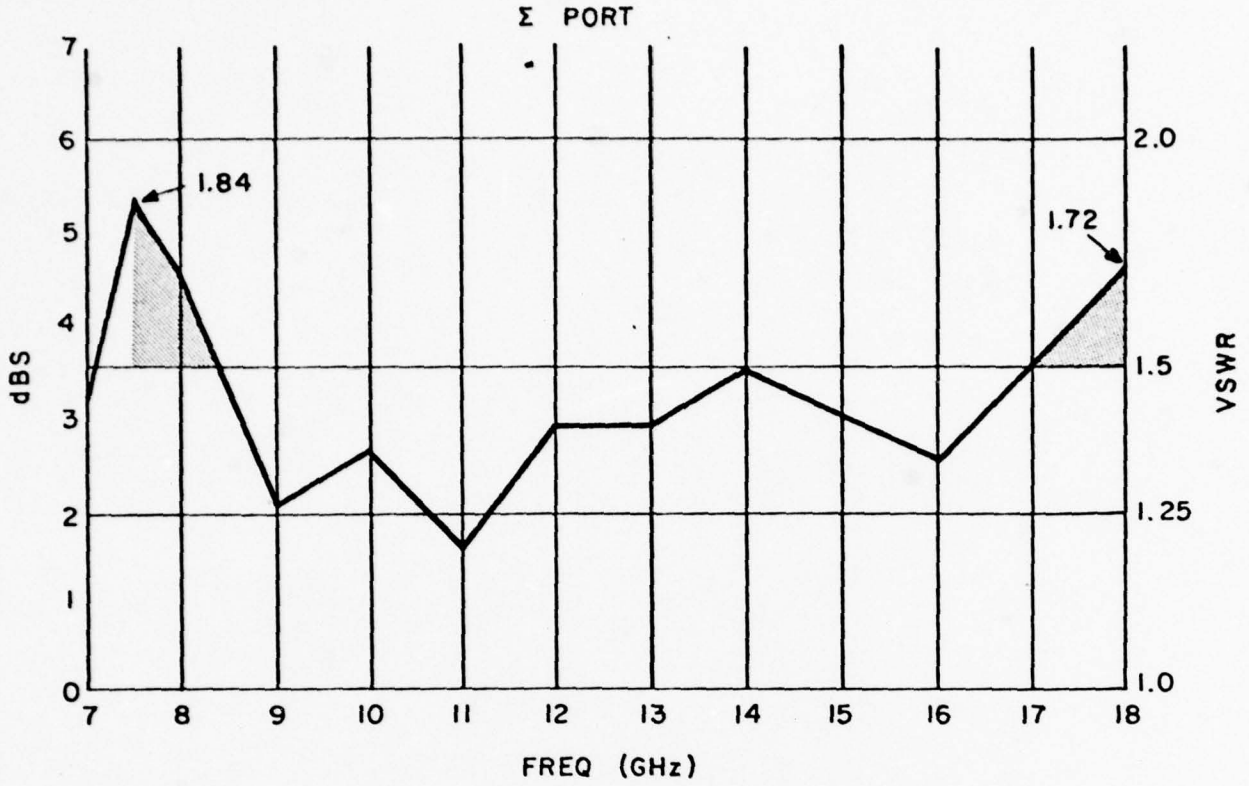

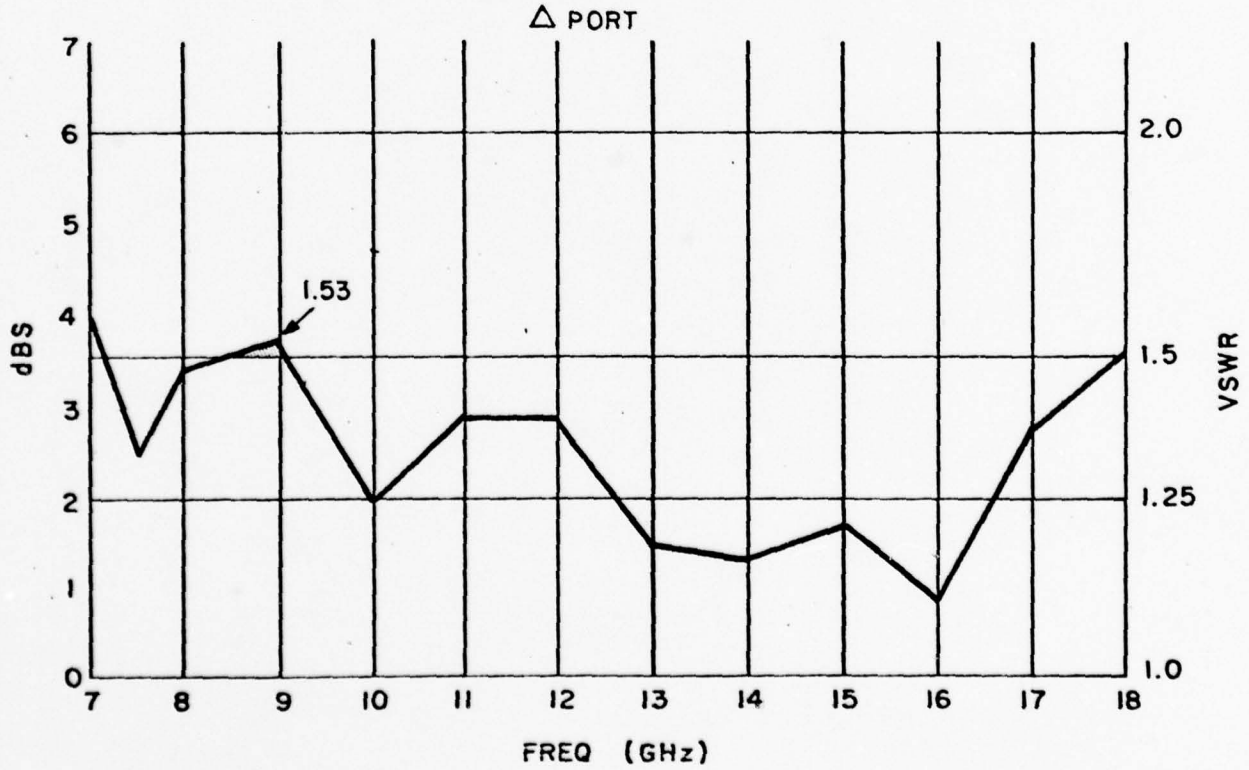

FIGURE 10 - Aluminum Hybrid 7-8 Brazed VSWR Data

formance would improve to better than 1.50:1, while its low end VSWR would change from 1.64:1 to 1.74:1.

E. Final Test Data

The final aluminum prototype design "Aluminum Hybrid 5-6 Septum Four", was also tested to determine, its amplitude split, phase split, insertion loss, isolation and power handling capability prior to shipment. Some minor deviations were required from the original specification.

LIST OF ORIGINAL SPECIFICATIONS AND CHANGES

(1) VSWR 1.5:1 (max.):	Change to less than 1.55:1 over 80% of Frequency Band; less than 1.75:1 over 100% of Frequency Band.
(2) Power Split ± 0.2 dB:	Unchanged
(3) Insertion Loss (max.) 0.5 dB:	Change to (max.) 0.5 dB from 7.5 to 17 GHz; 0.8 dB from 17 to 18 GHz.
(4) Isolation (min.)	
a. (sum to difference port) 30 dB:	Unchanged
b. (colinear to colinear) 15 dB:	Change to 14 dB
(5) Deviation of phase from theoretical ± 2°:	Change to ± 3°
(6) Frequency 7.5 through 18 GHz inclusive:	Unchanged
(7) Inputs/outputs to be compatible with WRD750D24 waveguide	Unchanged
(8) Power Level (CW) 1 Kw (pulsed) 10 Kw peak 1 Kw average	Unchanged

The VSWR of the sum and difference ports is given in Figure 8 in Section III-D above. The peak VSWR in the sum port was 1.64:1 while 80% of the band was less than 1.53:1. The peak VSWR of the difference port was 1.59:1 while 80% of the band was

less than 1.50:1. The VSWR of the colinear arms is shown in Figure 11. The peak VSWR of the colinear arms is 1.38:1 and typically better than 1.25:1.

The power split was within ± 0.2 dB. Swept data across the frequency band is given in Appendix A.

The insertion loss of the hybrid was less than 0.5 dB max. from 7.5 to 17 GHz, with a large portion of that band showing less than 0.2 dB loss. The maximum loss of 0.8 dB occurred at the extreme high end of the band. Swept data is given in Appendix A.

The sum to difference isolation of the hybrid was better than 30 dB. The colinear to colinear isolation was typically better than 15 dB with a peak value of 14 dB. Swept data is given in Appendix A.

The phase balance to the colinear arms was measured from the sum port using a 0° reference and from the difference port using a 180° difference. The phase split was within ±2 degrees over the entire band. Swept data is given in Appendix A.

The above parameters were tested over the entire 7.5 to 18 GHz band inclusive. VSWR was measured on a slotted line using a point-by-point method. All other measurements were done on a swept basis and that data is included in Appendix A.

The aluminum prototype hybrid is compatible with a standard WRD750D24 interface.

The hybrid was tested at 9.375 GHz with a 1 microsecond pulse transmitter. A level of 10 Kilowatts was applied to both the sum and difference ports for a period of 10 minutes each. No evidence of high reflection or arcing was noted.

In addition to the aluminum prototype hybrid supplied as line item 0001 of the original contract, a brassboard hybrid was supplied as line item 0003 of the ammended contract. VSWR data for the brassboard Step 30 hybrid is given in Figure 12.

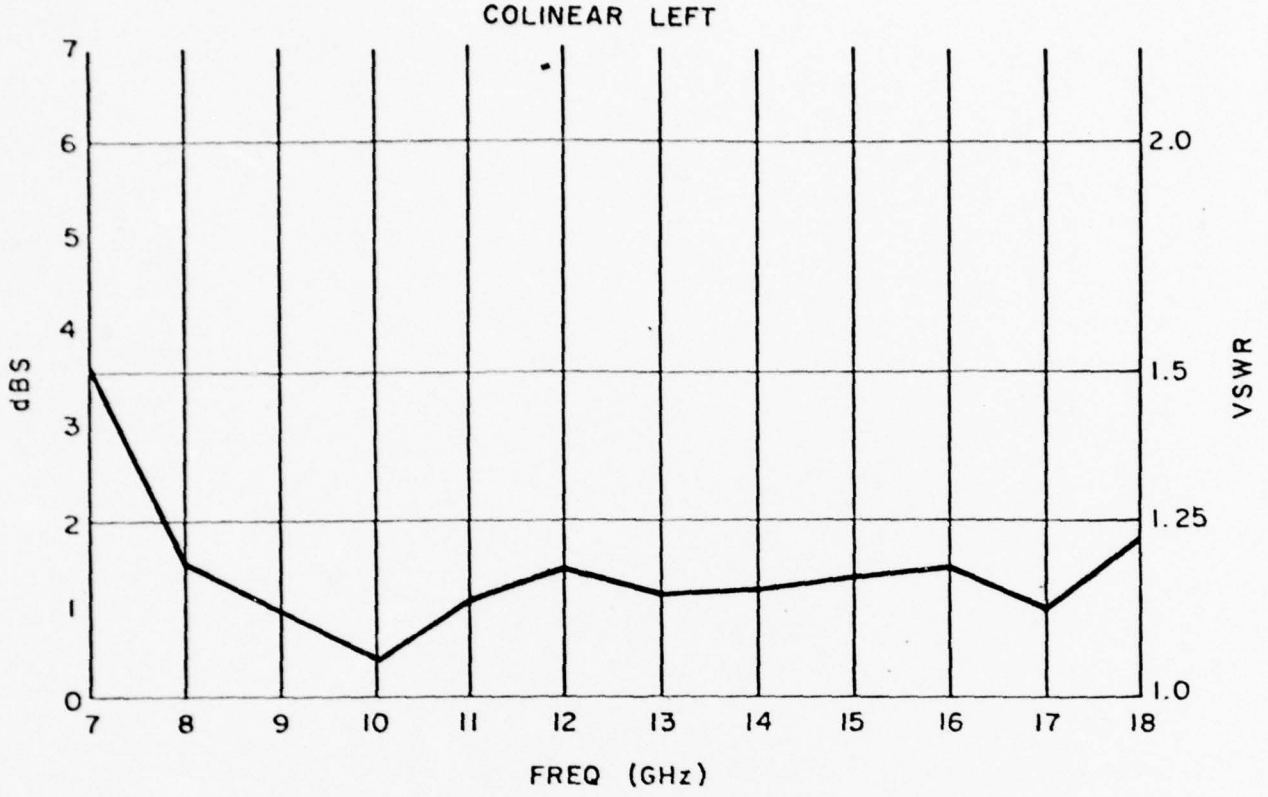

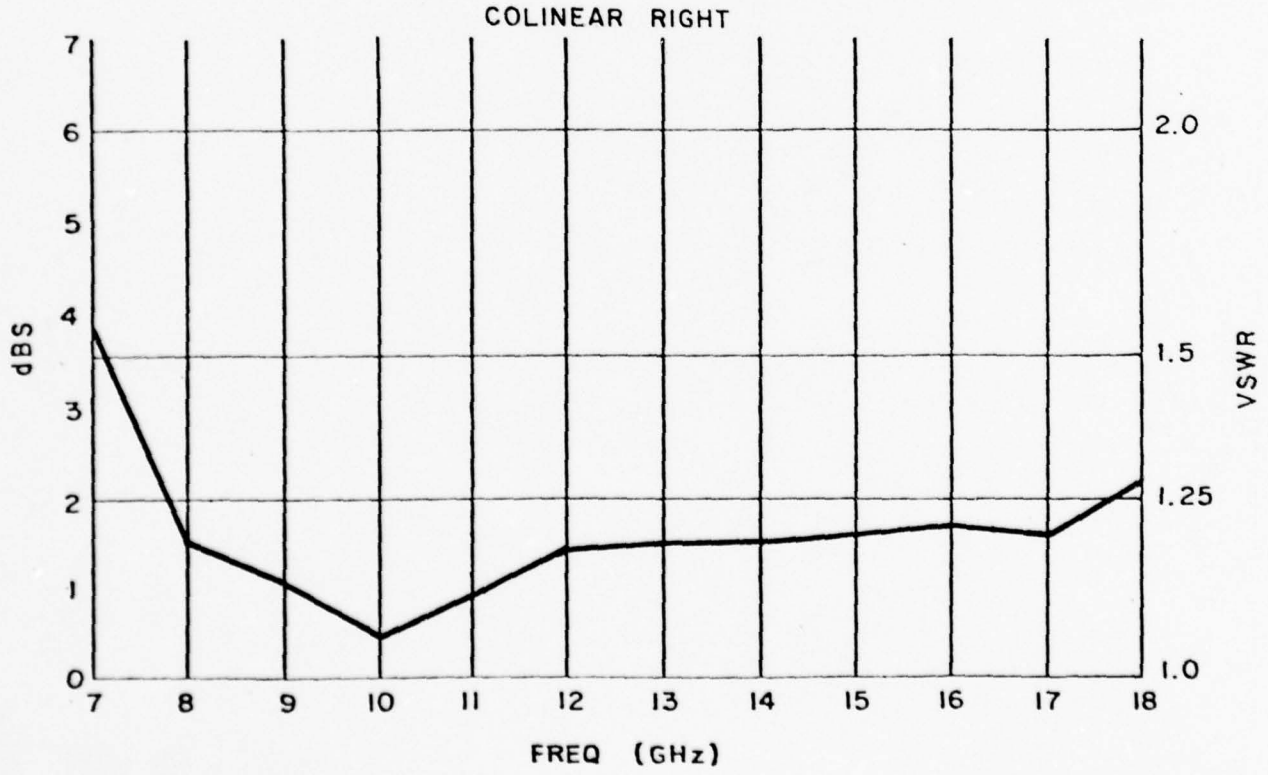

FIGURE 11 - Aluminum Hybrid 5-6 Colinear VSWR Data

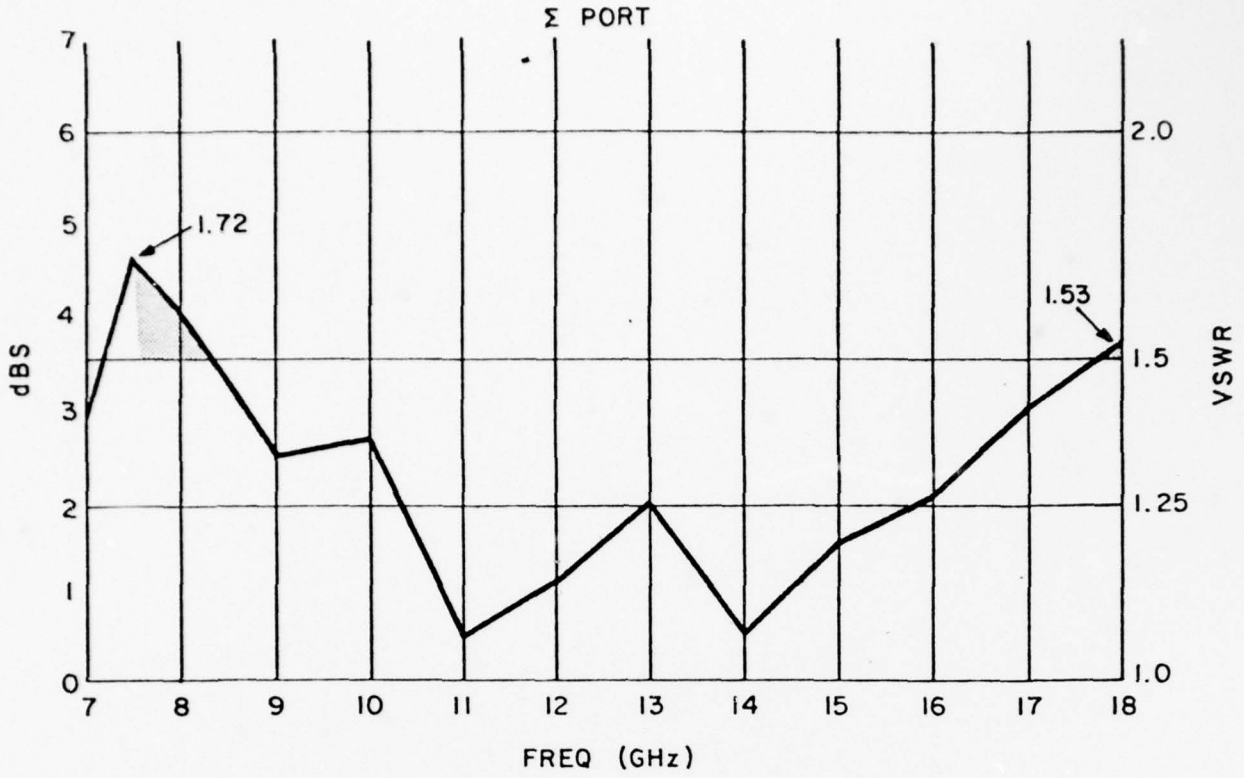

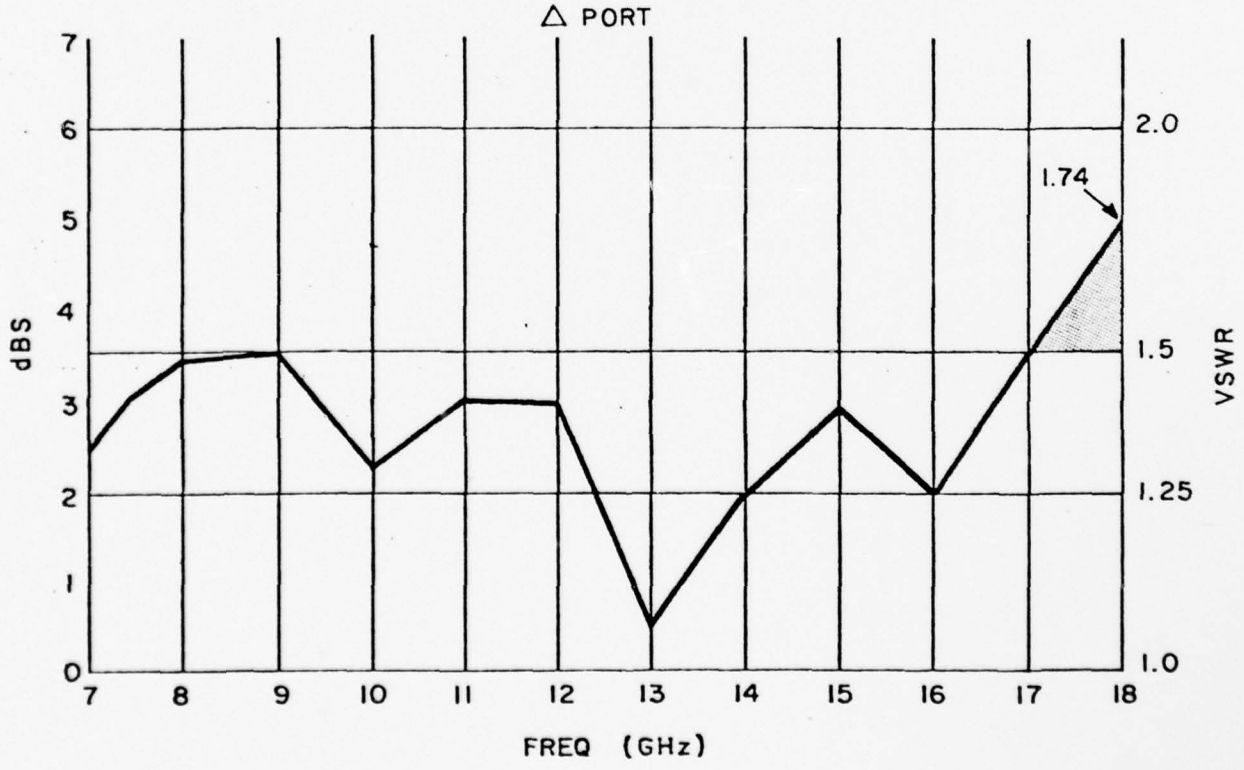

FIGURE 12 - Final Brassboard VSWR Data (Step 30)

The peak VSWR of the brassboard is 1.74:1 at the high end of the band in the difference port and 1.72:1 at the low end of the band in the sum port. The VSWR is less than 1.5:1 over more than 80% of the frequency band.

III. ANALYSIS OF HYBRID APPLICATION TO MATRIX

A. MATRIX OPERATION

High power broadband waveguide matrices are used as output and input matrices in a high power four throw switch matrix. The matrix approach allows the switching of high RF power levels with a minimum of dissipated power. The design of the network is such that no high level RF power passes through any diode or ferrite device. These devices are not only the main source of dissipation in conventional switching devices, but also the main cause of power handling limitations.

Figure 1 shows the schematic diagram of the high power four throw switch matrix. The overall network consists of a low power four throw diode switch, a four port input matrix, four high power TWTA's and a four port output matrix. For the purpose of this description of the matrix operation, it will be assumed that the TWT's are perfectly phase-matched, and that the phase distribution applied at low power lines 1, 2, 3 and 4 is faithfully reproduced at high power lines 1, 2, 3 and 4 respectively.

The diode switch applies low level RF input power (sufficient power to drive TWT's) to one of four inputs of the input matrix. The matrix consists of four ridgeguide magic tee hybrid junctions interconnected as shown schematically in the left hand portion of Figure 1, and pictorially in Figure 13.

Input terminals 1 and 2 are the difference and sum ports of hybrid B (See Figure 1), and input terminals 3 and 4 are the difference and sum ports of hybrid A. The colinear arms of hybrid B are connected to the sum ports of hybrids C and D via a pair of equal length lines. The colinear ports of hybrid A are connected to

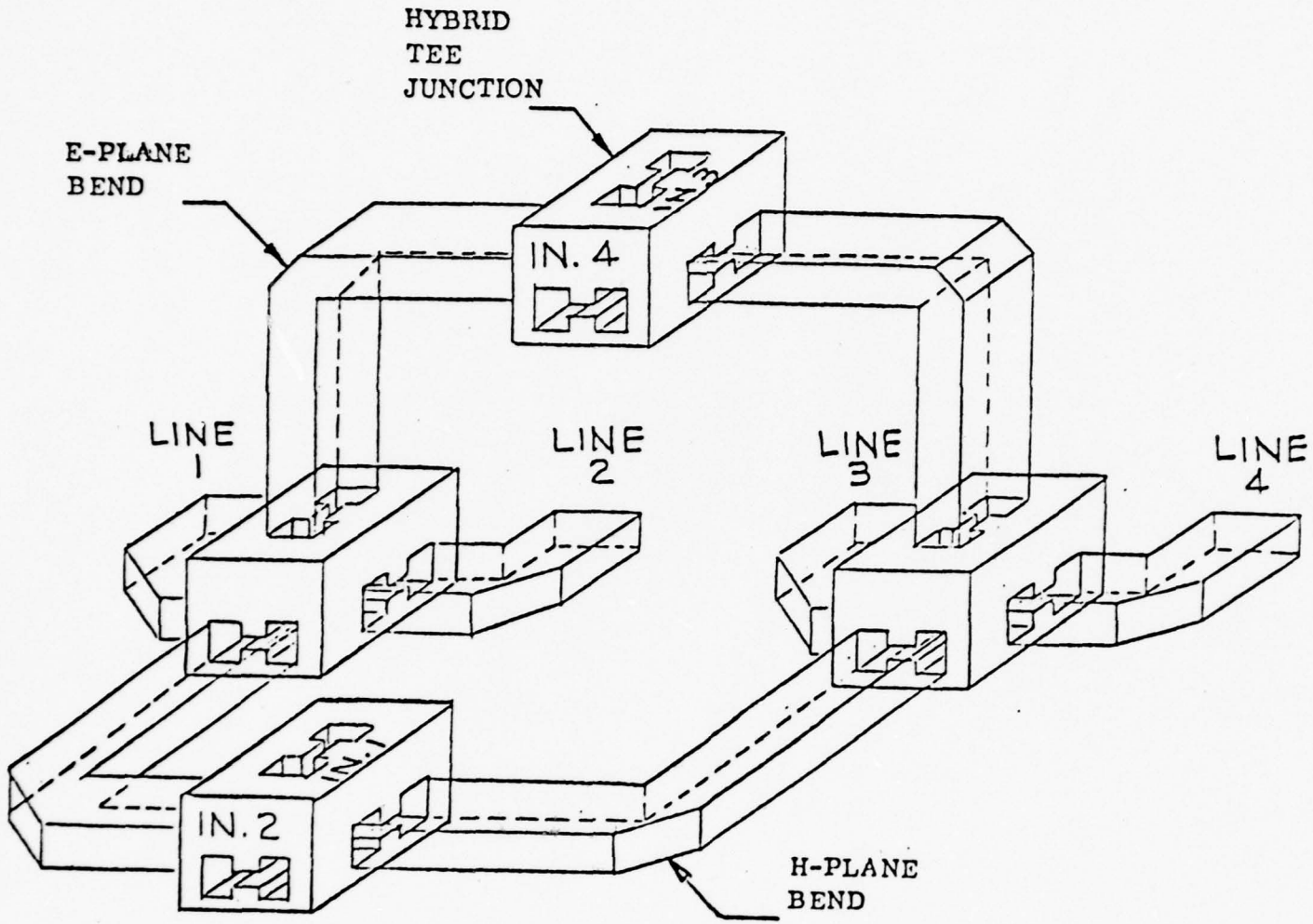

FIGURE 13 PHYSICAL CONFIGURATION, FOUR PORT RIDGE WAVEGUIDE MATRIX

the difference ports of hybrids C and D via a second pair of equal length lines. (It will be demonstrated in Section II-B that certain pairs of lines can be made asymmetrical while still preserving overall phase coherence.)

The output four port matrix is identical to the input four port matrix making the network (neglecting the tubes) perfectly symmetrical. The equivilance of hybrids is as follows:

H ⟷ A F ⟷ C

G ⟷ B E ⟷ D

Since the matrices are lossless (theoretically), reciprocal networks, a signal applied to a given input port will apply the proper phase taper on the interface lines for transmission to the equivalent output port.

For example, a signal applied at input terminal 3 (the difference port of hybrid A) will split in an anti-phase condition between the colinear arms of hybrid A. Consequently anti-phase signals will be applied to the difference ports of hybrids C and D. Hybrid C will apply anti-phase signals on interface lines 1 and 2 resulting in an output at the difference port of Hybrid E. Hybrid D will produce anti-phase signals on lines 3 and 4 resulting in an output from the difference port of hybrid F. These outputs are applied to the colinear arms of hybrid H. However, these signals are out of phase with each other due to the initial anti-phase split at hybrid A. Consequently the output signal will appear at the difference port of hybrid H, which is output terminal 3 of the overall matrix.

The only junctions which must handle the combined output power of four tubes are the sum and difference ports of hybrids G and H. Hybrids E and F need handle only the power output of two tubes.

Although hybrids A, B, C and D handle only the low drive power required by the tubes, they are constructed identically to hybrids E, F, G and H. This insures perfect symmetry in the high power four throw switch matrix.

B. DETAILED DESIGN CONSIDERATIONS

The four port matrix should have a peak VSWR of 2.2:1 in the four "terminal" ports. The "terminal" ports are the input ports in the case of the low power matrix, and the output ports in the case of the high power matrix. The "line" ports are those which would connect with the TWT amplifiers as shown in Figure 1.

As can be seen in Figure 13 a four port matrix consists of two layers of hybrid tee junctions. Consequently, the VSWR seen at a terminal port will be the resultant of the interaction of two hybrid tee VSWR's. The worst interaction of VSWR's occurs in the terminal ports 2 and 3 where there is a coherent relationship between two hybrid tee sum ports and between two hybrid tee difference ports. When the hybrids are designed to be identical to each other, all of the sum ports will have a peak VSWR at the same frequency, as will be the case for all of the difference ports. When two VSWR's "add" in-phase coherently, the resultant is their product (actually it is the dB SWR's which add). When they combine out-of-phase coherently, the resultant is their quotient. Consequently two 1.5:1 VSWR's could produce as much as a 2.25:1 VSWR and as little as 1:1 (perfect match).

The possibility of in-phase VSWR interactions would require that each hybrid have a maximum VSWR of slightly less than 1.5:1 in order to insure that the four port matrix would have a VSWR of under 2.2:1. However, several approaches are available to allow the use of hybrids with <u>peak</u> VSWR's greater than 1.5:1 provided that the <u>typical</u> VSWR remains under 1.5:1 over most of the frequency band. These

are listed below:

1. Symmetrical Line-Length Adjustment

This approach depends on the peak VSWR of hybrid occurring over a very narrow portion of the frequency band. Referring to Figure 14, which is a schematic representation of Figure 13 it can be seen that for coherent symmetrical operation it is necessary that:

$$\ell 5 = \ell 6$$

$$\text{and } \ell 7 = \ell 8$$

$$\text{and } \ell 1 = \ell 2 = \ell 3 = \ell 4$$

As a result, the sum port reflections of hybrids C and D will add coherently at the colinear arms of hybrid B ($\ell 7 = \ell 8$). Their combined effect will be that of another single sum port connected by a length of line with the sum port of hybrid B. Consider now, the case where the sum ports of hybrids B, C and D all have an identical VSWR characteristic with a peak value of 1.7:1 over a very narrow portion of the frequency band. If the length of lines 7 and 8 is such that the 1.7:1 VSWR from the combined C and D sum ports produces a reflection phase which adds with the 1.7:1 VSWR from the hybrid B sum port, a resultant VSWR of 2.89:1 will occur at terminal port 2 of the matrix.

Now if equal length ridge waveguide shims are added in both lines 7 and 8, the effective combined VSWR of sum ports C and D will still be 1.7:1, but the phase of the reflection coefficient, as seen at sum port B will be changed. The resultant VSWR will be less than 2.89:1. The exact resultant VSWR for an interaction of arbitrary phase can be calculated from the following equation:

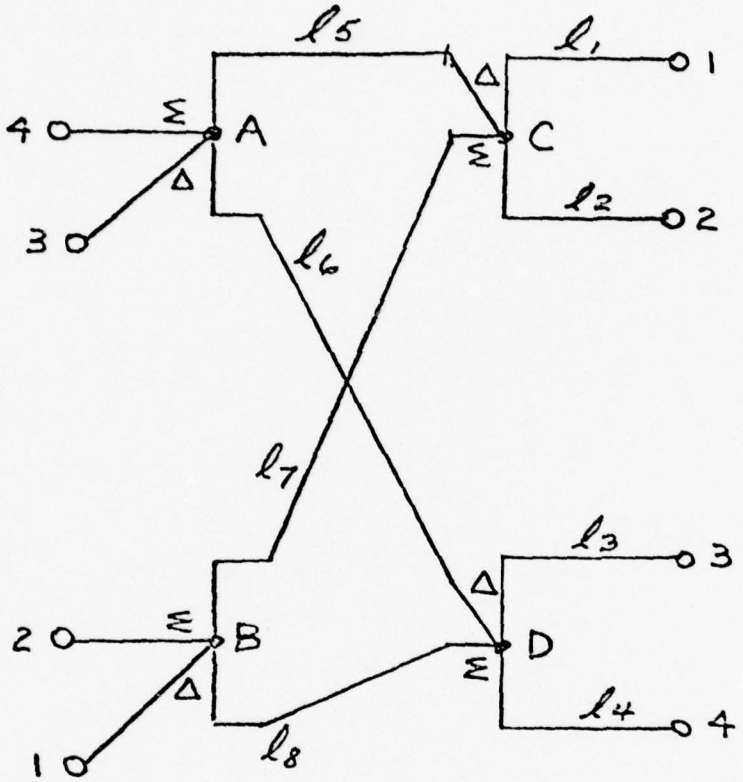

FIGURE 14 - Connections Within a Four-Port Matrix

(equa. 1) $$V_T = \frac{1 + |R_T|}{1 - |R_T|}$$

where V_T is the terminal VSWR and R_T is the total reflection as given by the following equation:

(equa. 2) $$R_T = R_B + \frac{R_{CD}\, e^{j\phi}\, (1 - R_B^2)}{1 + R_B R_{CD}\, e^{j\phi}}$$

R_B is the voltage reflection coefficient from the sum port of hybrid B while R_{CD} is the resultant reflection from hybrids C and D. Exp j ϕ is the phase shift introduced by lines 7 and 8.

(equa. 3) $$\phi = 360^\circ \left(\frac{2\ell}{\lambda g}\right)$$

In the case of small reflections, equation 2 may be simplified to form equation 4 as follows:

(equa. 4) $$R_T = R_B + R_{CD}\, e^{j\phi}$$

The approximation of equation 4 is still fairly valid for a pair of VSWR's equal to 1.7:1 (reflection coefficients of 0.259). E.g.: If equations 2 and 1 are used, $R_T = 0.485$ and $V_T = 2.883{:}1$, while if equations 4 and 1 are used, $R_T = 0.518$ and $V_T = 3.149{:}1$. If $\phi = 0$, the worst case error given above occurs; if $\phi = \pi$, the approximation of equation 4 is exact because $R_B = R_{CD}$.

Now, using the approximation of equation 4, which gives a pessimistic result, let us assume that we wish to hold V_T to under 2.2:1 and R_T to under 0.375 with a 1.7:1 hybrid VSWR. ($R_B = R_{CD} = 0.259$)

Substituting in equation 4, we have:

(equa. 5) $$0.375 \geq 0.259 \left| 1 + e^{j\phi} \right|$$

which becomes

(equa. 6) $$\frac{0.375}{0.259} = 1.448 \geq 2 \cos \left(\frac{1}{2} \phi\right)$$

(equa. 7) $$87.2^\circ \leq \phi \leq 360^\circ - 87.2^\circ$$

Consider now a case where the lengths of lines 7 and 8 are both 10 inches. Using 1.876 inches for the cut-off wavelength of WRD750D24 ridge waveguide, the guide wavelength at 7.5 GHz is 2.889 inches and the guide wavelength at 8.0 GHz is 2.387 inches. The round-trip phase through a 10 inch length, as given by equation 3, is 2472 degrees at 7.5 and 3016 degrees at 8.0 GHz, corresponding to a change in electrical length of 524 degrees over a 500 MHz bandwidth. Reviewing equation 7, it can be seen that the cancellation of reflection coefficients is only adequate over a 185 degree range. Consequently, this cancellation technique would only be effective over about a 177 MHz range. If the absolute lengths of lines 7 and 8 were only 5 inches, then the technique of symmetrical shims placed in both lines would work over twice that bandwidth.

2. Non-Symmetrical Line-Length Adjustment

Another technique of avoiding a worst case interaction of VSWR's is to shim the lines within a matrix in a non-symmetrical fashion. Referring to Figure 14,suppose that a quarter wave shim is placed in lines 1, 2, 6 and 8. The overall transmission phase from any one terminal port to the four line ports will remain balanced. However, the round trip phase between hybrid junctions will be different by a half wave. When terminal 2 is used as the input port, the signal reflected from the sum ports of hybrids C and D will tend to return to the difference port of B rather than the sum port. This will prevent an addition of R_B and R_{CD} at terminal port 2. For the case of perfect cancellation (exact quarter wave shims), the

reflection seen at port 2 will be equal to just the sum port reflection of hybrid B. It should be pointed out however, that the isolation between terminal ports 2 and 1 does become deteriorated. In the case described above, the isolation becomes approximately equal to $|R_{CD}|$.

The bandwidth of this technique is greater than for the symmetrical line-length adjustment because it depends on the differential length between lines 7 and 8 rather than upon their gross length. In WRD750D24, a shim chosen to exactly 0.250 λg at 7.5 GHz would be 0.722 inches thick; this same shim would be 0.303 λg at 8.0 GHz. The round-trip phase through this shim would be 180 degrees at 7.5 and 218 degrees at 8.0 GHz.

Now let us consider the amount of round-trip phase variation which is tolerable in this approach. Assuming that the gross insertion phase, ϕ, could take on any value, the results of equation 4 must be used as follows:

(equa. 8) $$|R_T| \geq |R_B| + |R_{CD}|$$

In the case of maintaining a 2.2:1 VSWR at terminal 2, with sum port VSWR's of 1.7:1, this requires that:

(equa. 9) $$0.375 \geq 0.259 + |R_{CD}|$$

(equa. 10) $$|R_{CD}| \leq 0.116$$

Assuming that $R_C = R_D$, their resultant effect at sum port B is given by:

(equa. 11) $$R_{CD} = R_C \cos \frac{1}{2}\theta$$

Where θ is the round-trip phase through the shim of thickness S given by:

(equa. 12) $$\theta = 360° \left(\frac{2S}{\lambda g}\right)$$

Substituting into equation 11,

(equa. 13) $.116 \geq .259 \cos \frac{1}{2} \theta$

(equa. 14) $126° \leq \theta \leq 360° - 126°$

This leads to the conclusion that the non-symmetrical line-length adjustment technique will work for round-trip phase values between 126 degrees and 243 degrees.

Furthermore, the technique can be applied in the frequency region where the quarter wave shim becomes three-quarter guide wavelengths thick, where θ is between 486 degrees and 594 degrees. Thus if a shim is chosen to obtain $\theta = 126$ degrees at 7.5 GHz (S = 0.506 inches), it will produce 234 degrees at 9.85 GHz. The same shim will also produce 486 degrees at 16.95 GHz. Therefore, the non-symmetrical shimming approach can be used to accommodate a 1.7:1 hybrid VSWR over a 2350 MHz range at the low end of the 7.5 to 18.0 GHz frequency band and over a 1050 MHz range at the high end of the band simultaneously.

3. Non-Identical Hybrid Junctions

Another technique of avoiding a peak VSWR of over 2.2:1 in the four port matrix is to utilize hybrid junctions which do not all have a peak VSWR at the same frequency. Suppose that the sum port of hybrid B has a 1.7:1 VSWR at 7.5 GHz. If the sum ports of hybrids C and D have a VSWR under 1.3:1 at 7.5 GHz, the resultant VSWR will remain under 2.2:1. Similarly, at 18 GHz, hybrids C and D can have a 1.7:1 VSWR if hybrid B has better than a 1.3:1 VSWR. This third approach does not readily lend itself to theoretical analysis. However, by reviewing the VSWR data for a large number of prototype hybrid designs, it has been concluded that this approach is probably of very limited value.

IV CONCLUSIONS AND RECOMMENDATIONS

The Broadband Magic Hybrid development conducted under Contract No. N00173-76-C-0335 for the Naval Research Laboratory by Sedco Systems has demonstrated the feasibility of building a high power, low loss, low VSWR device operating over the frequency range of 7.5 to 18 GHz. The development program not only led to a brassboard design but also included the fabrication of aluminum production prototypes which demonstrated the feasibility of applying the microwave design to practical hardware requirements. The resultant performance of the hybrid device was very close to that originally projected.

An analysis was conducted which demonstrated that the hybrid performance obtained in the course of this program was suitable for use in a four port waveguide matrix which could be used to combine the output of four high power traveling wave tube amplifiers. Since future systems application will require very high levels of power over very broad bandwidths, and since TWT amplifiers can provide moderately high power over these same bandwidths, it is recommended that a four port waveguide matrix be constructed using the WRD750D24 magic tee hybrid design which was developed as part of this program.

APPENDIX A

PERFORMANCE DATA

6-18-77

S/N 5-6

PHASE BALANCE

Σ PORT TO COLINEAR ARMS RED #5 GREEN #6

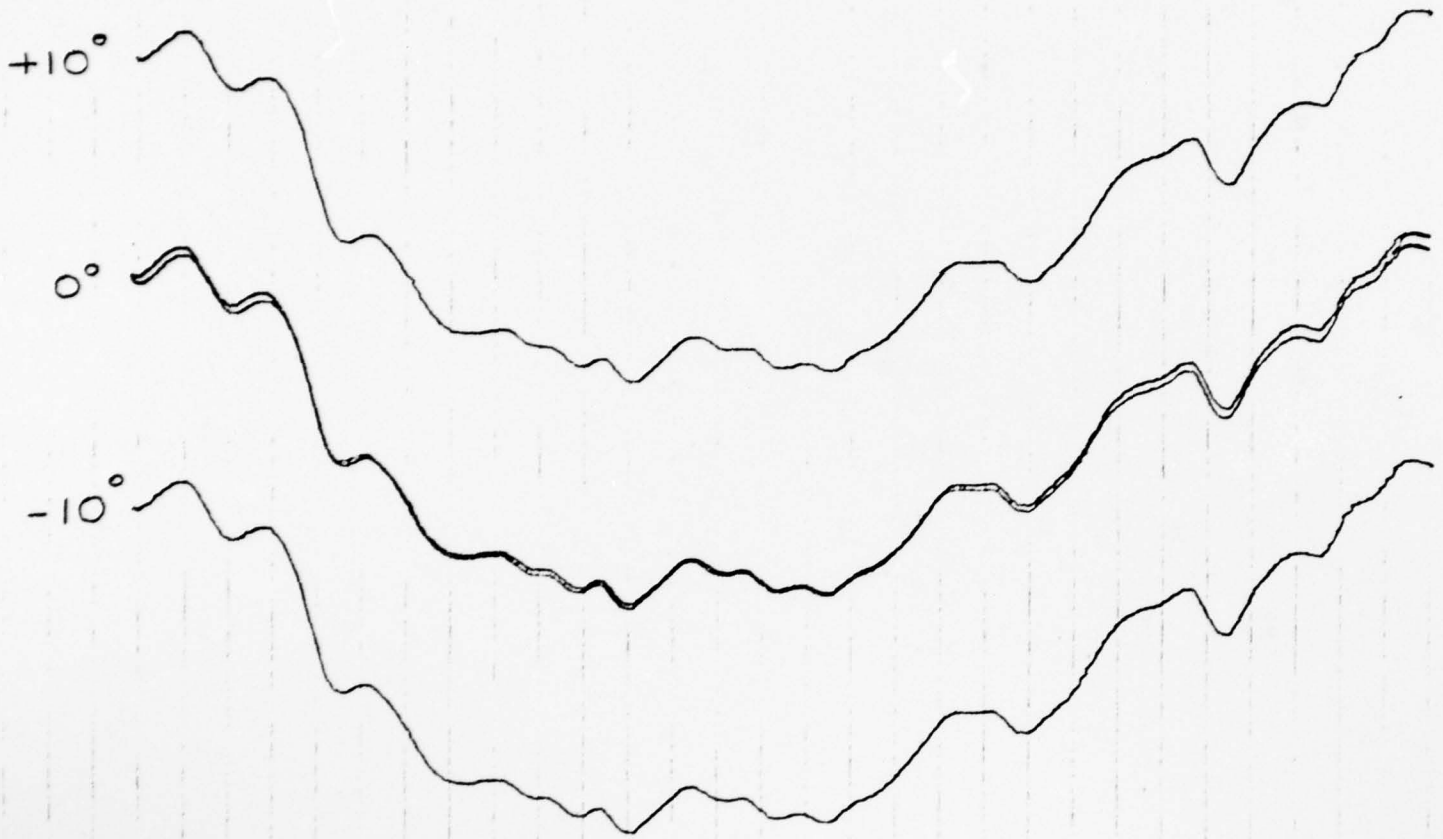

6-18-77

PHASE BALANCE

S/N 5-6

Σ PORT TO COLINEAR ARMS RED REF #5
GREEN #6

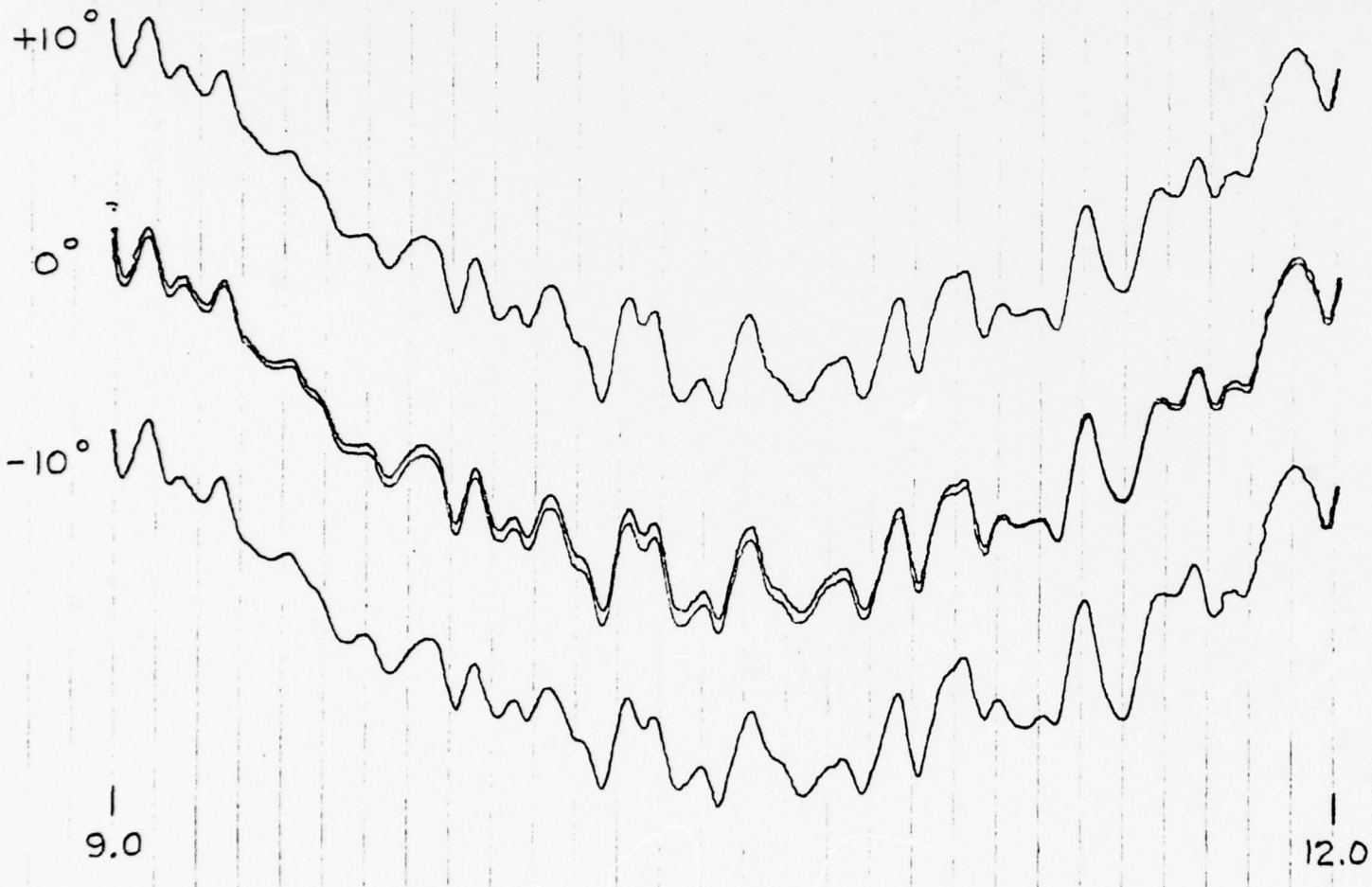

PHASE BALANCE

6-18-77

Σ PORT TO COLINEAR ARMS RED REF #5 GREEN #6

S/N 5-6

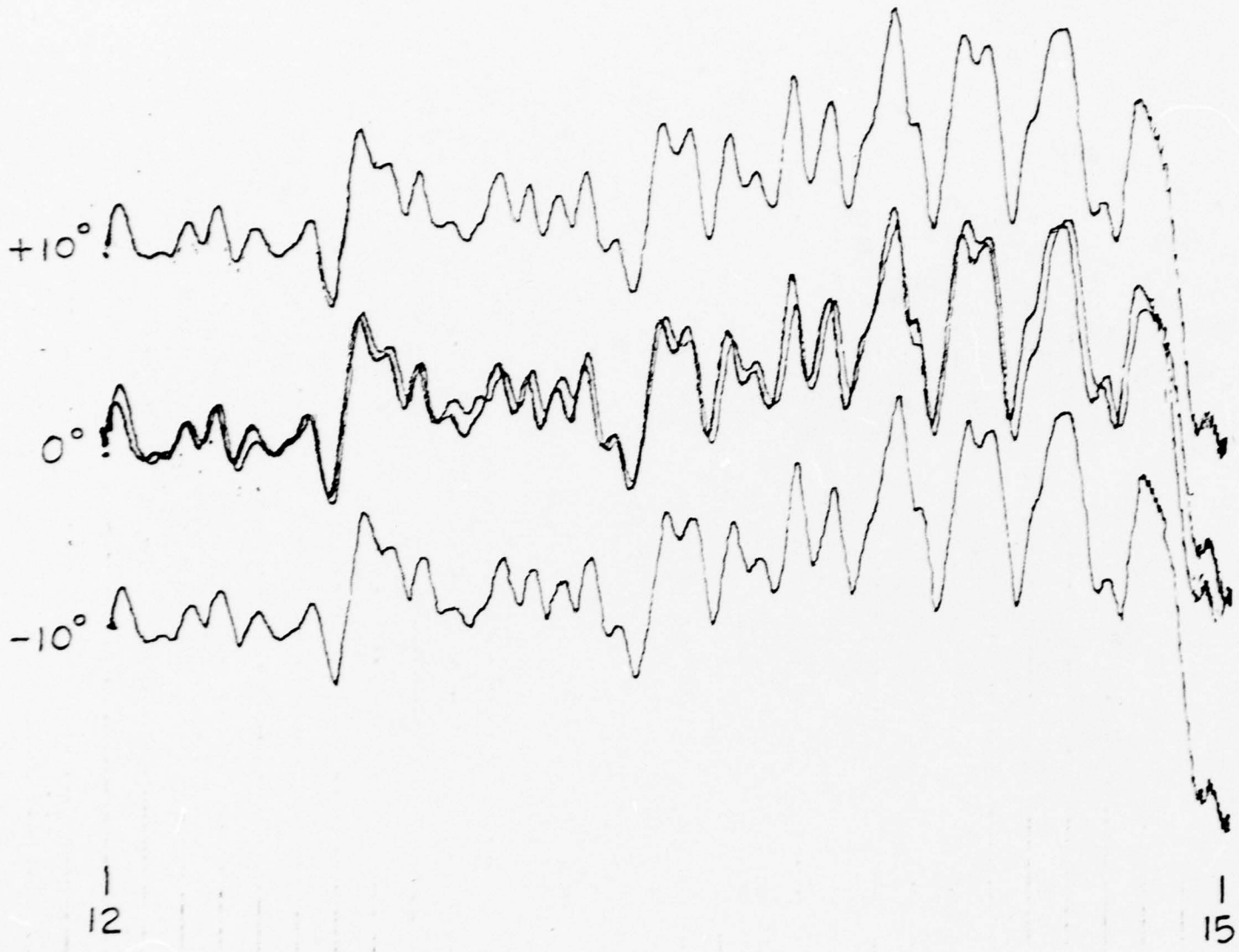

PAGE 13

6-18-77

PHASE BALANCE

S/N 5-6

Σ PORT TO COLINEAR ARMS RED REF #5
GREEN #6

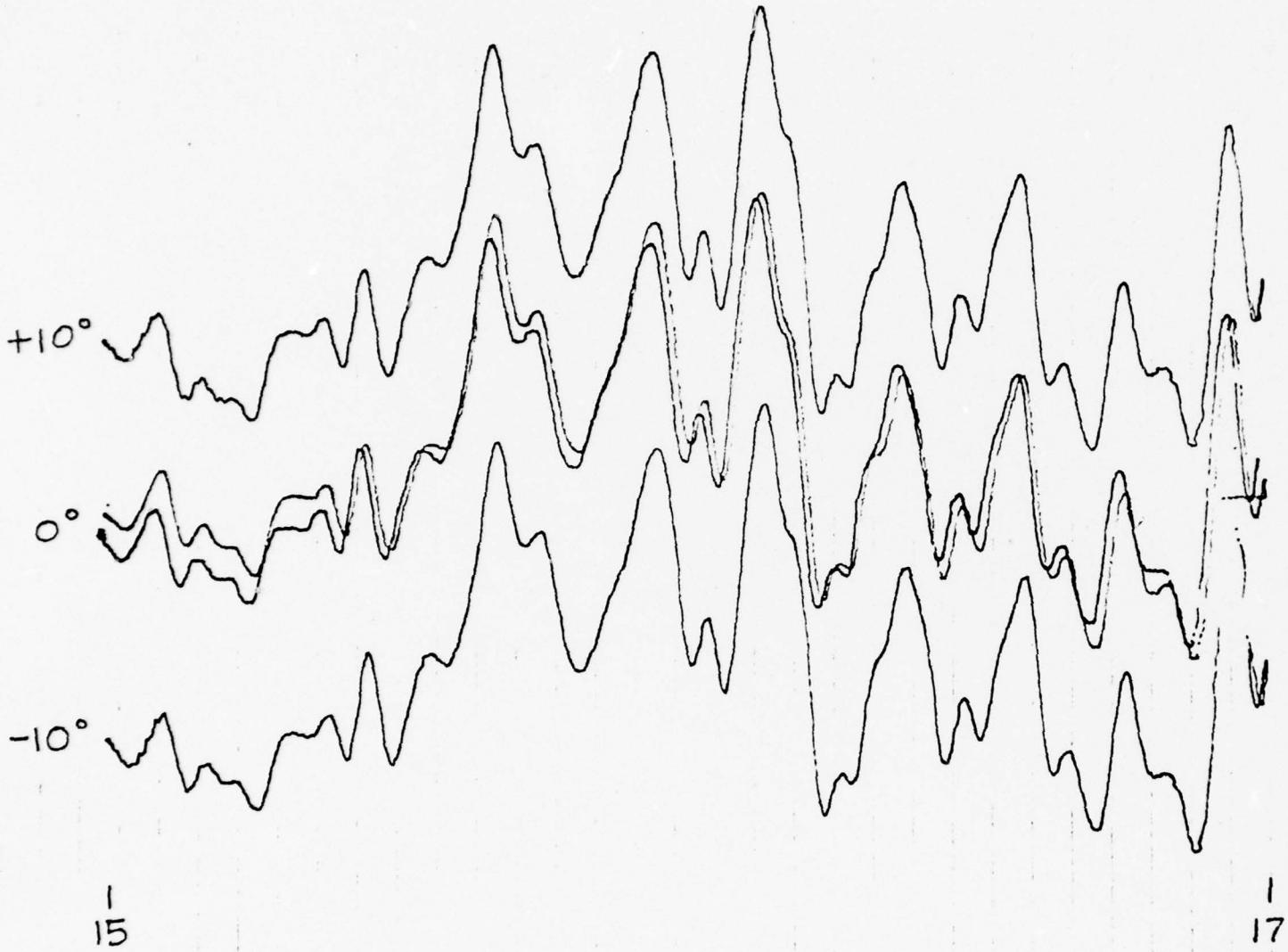

PHASE BALANCE

6-18-77

Σ PORT TO COLINEAR ARMS RED REF #5
GREEN #6

S/N 5-6

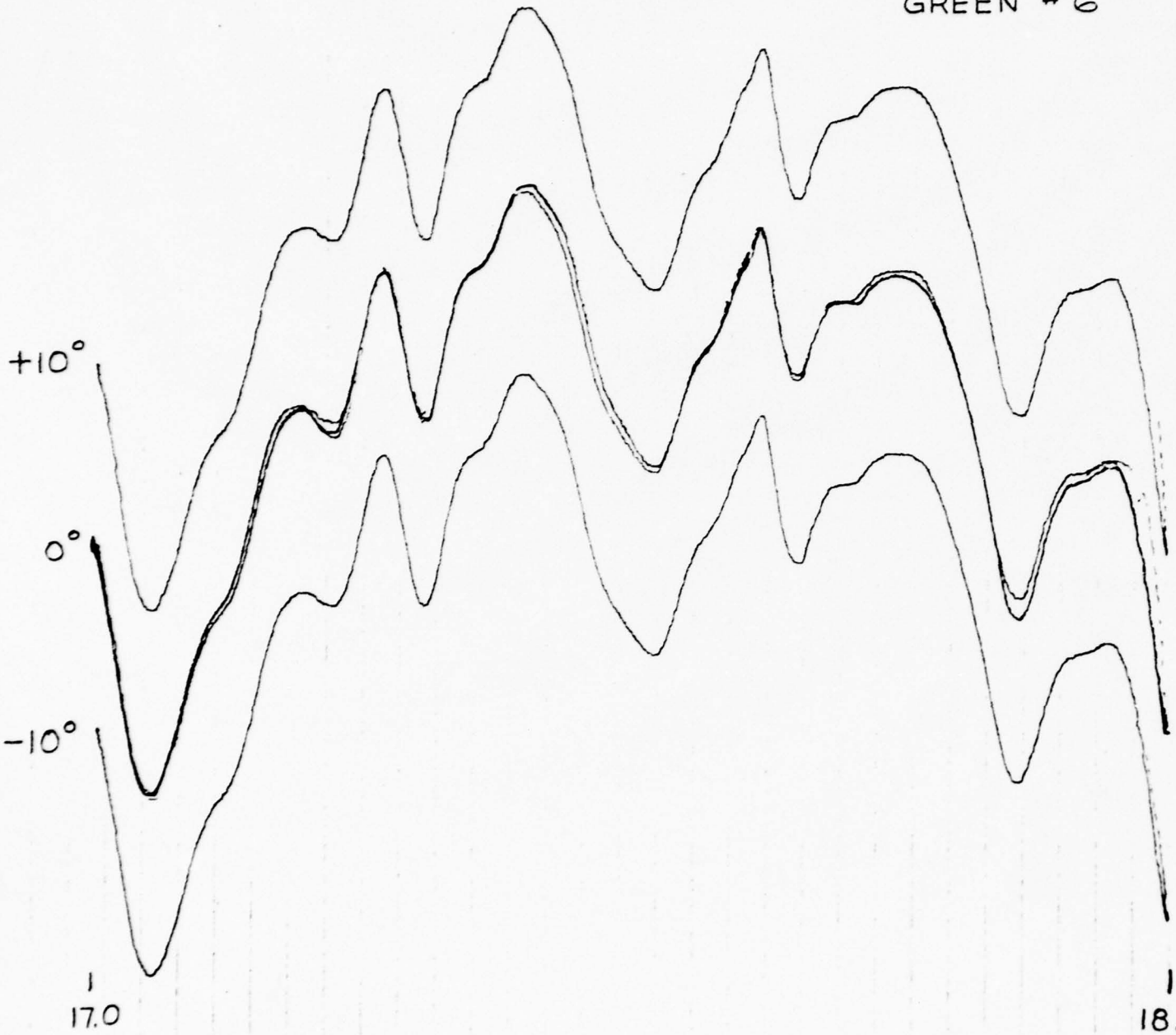

6-18-77

PHASE BALANCE

S/N 5-6

△ PORT TO COLINEAR ARMS

RED REF #5
GREEN #6

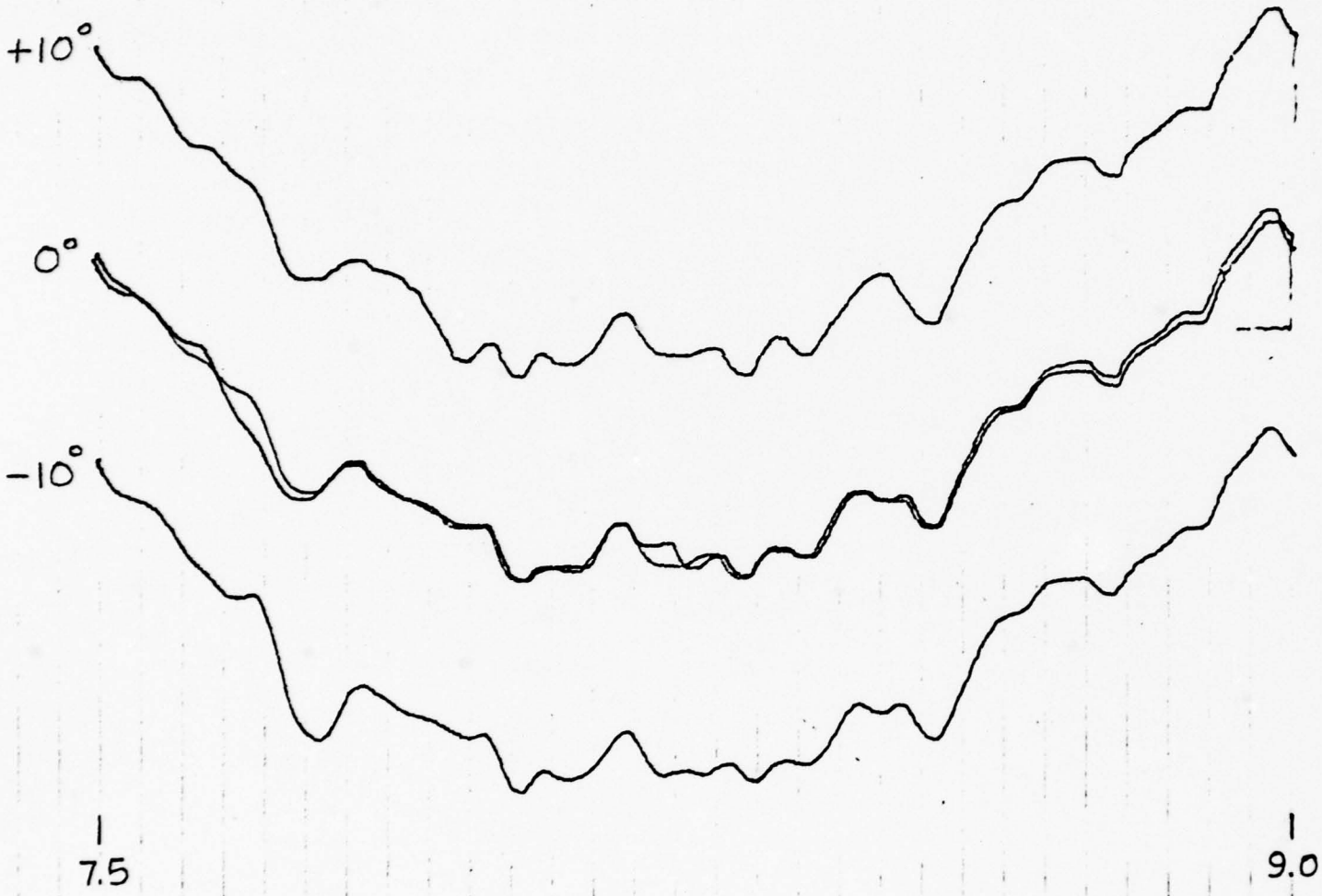

PAGE AG

6-18-77

S/N 5-6

PHASE BALANCE

△ PORT TO COLINEAR ARMS

RED REF #5
GREEN #6

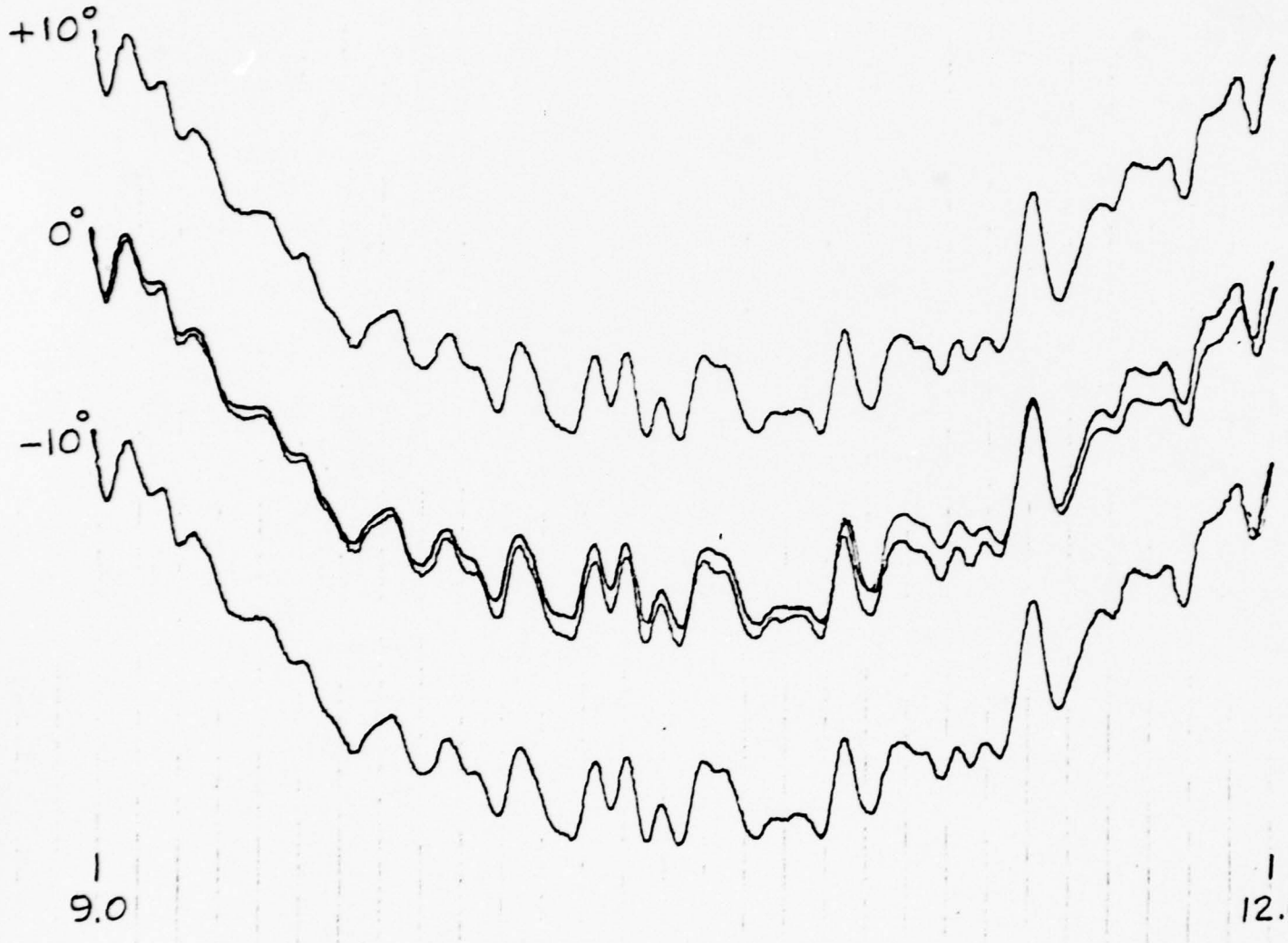

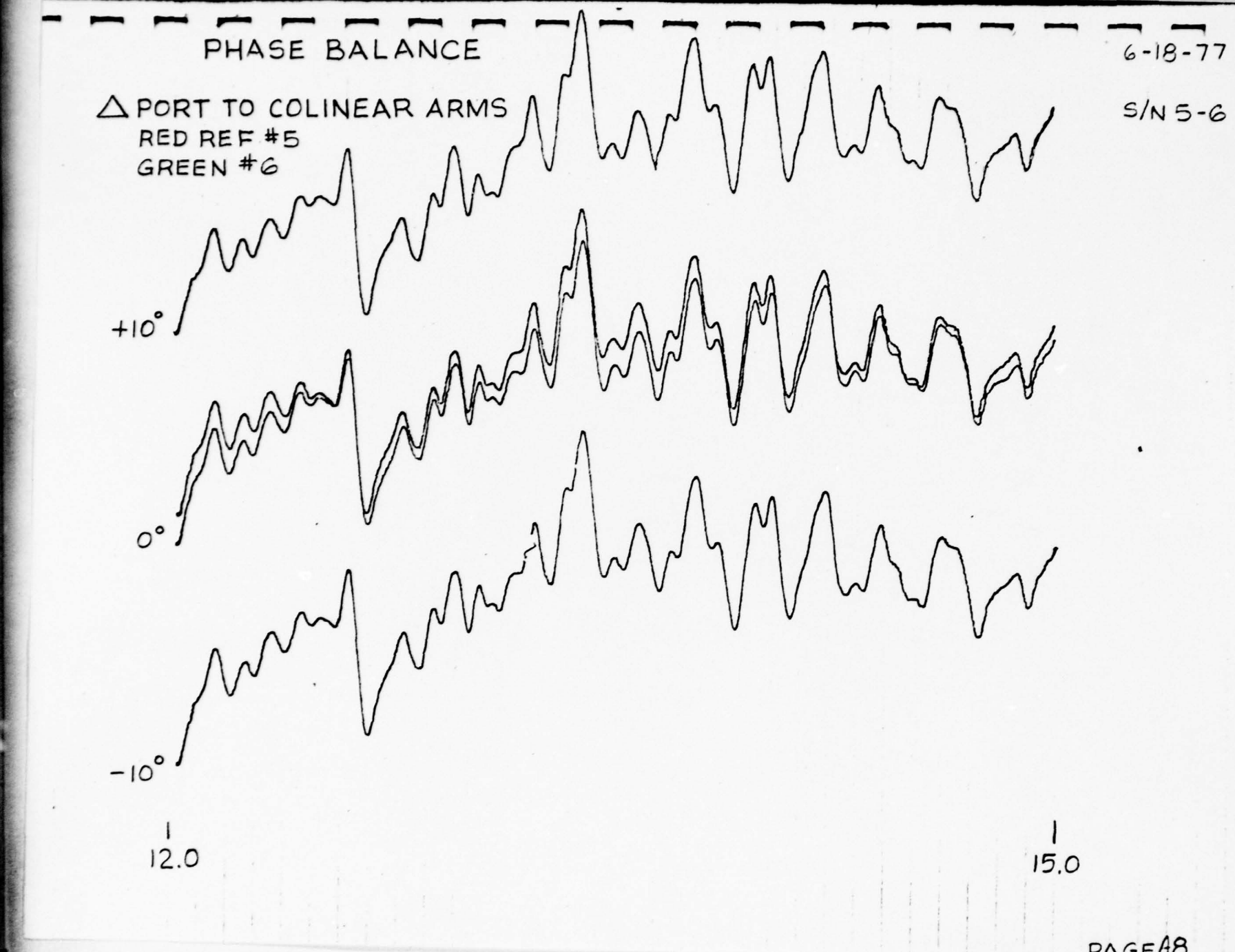
PHASE BALANCE
6-18-77
△ PORT TO COLINEAR ARMS
RED REF #5
GREEN #6
S/N 5-6
+10°
0°
-10°
12.0
15.0

6-18-77

PHASE BALANCE

S/N 5-6

△ PORT TO COLINEAR ARMS RED REF #5 GREEN #6

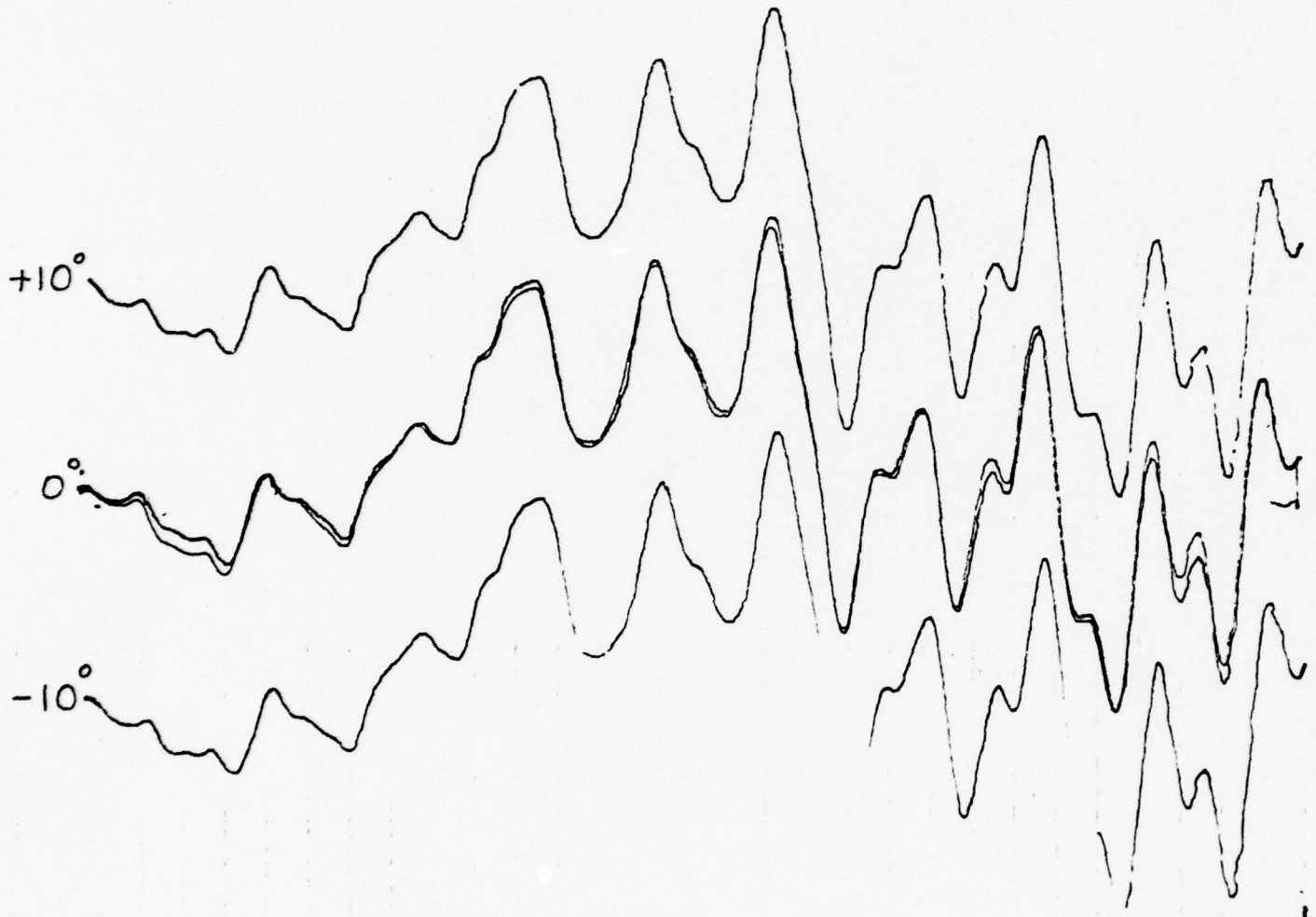

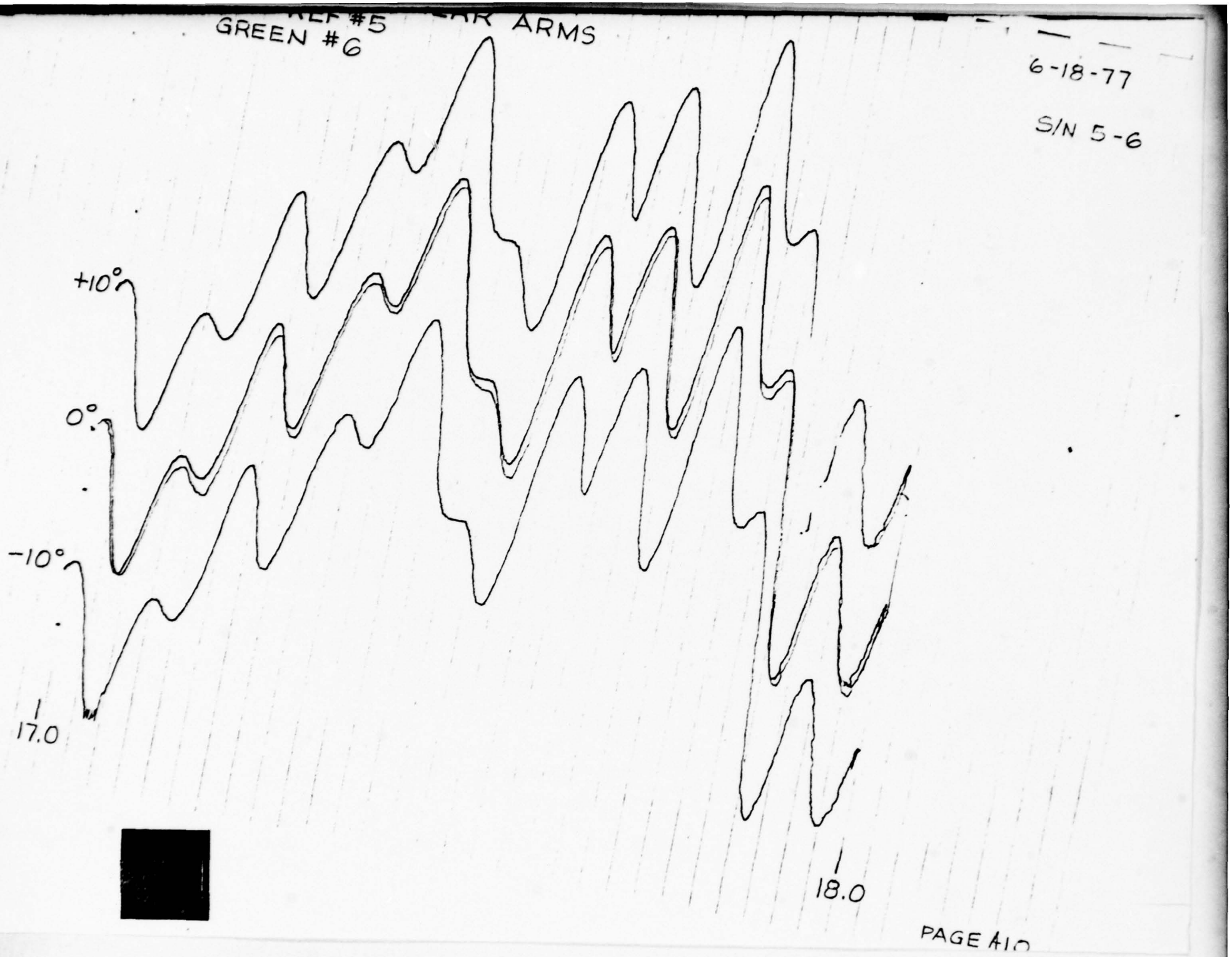
#5 ARMS
GREEN #6
6-18-77
S/N 5-6
+10°
0°
-10°
17.0
18.0

6-18-77

ISOLATION

S/N 5-6

Δ -Σ PORTS

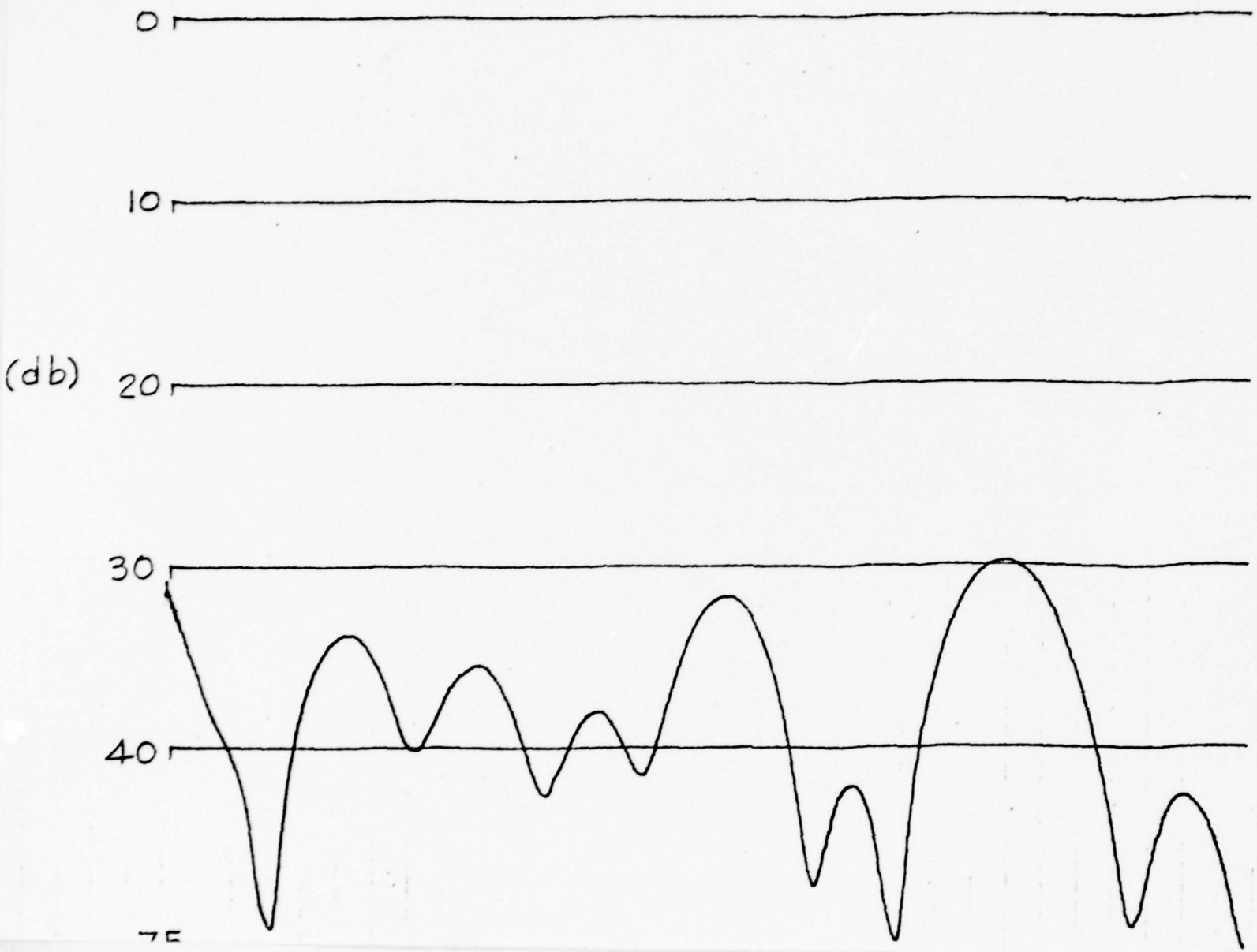

6·18·77

ISOLATION

S/N 5-6

Δ - Σ PORTS

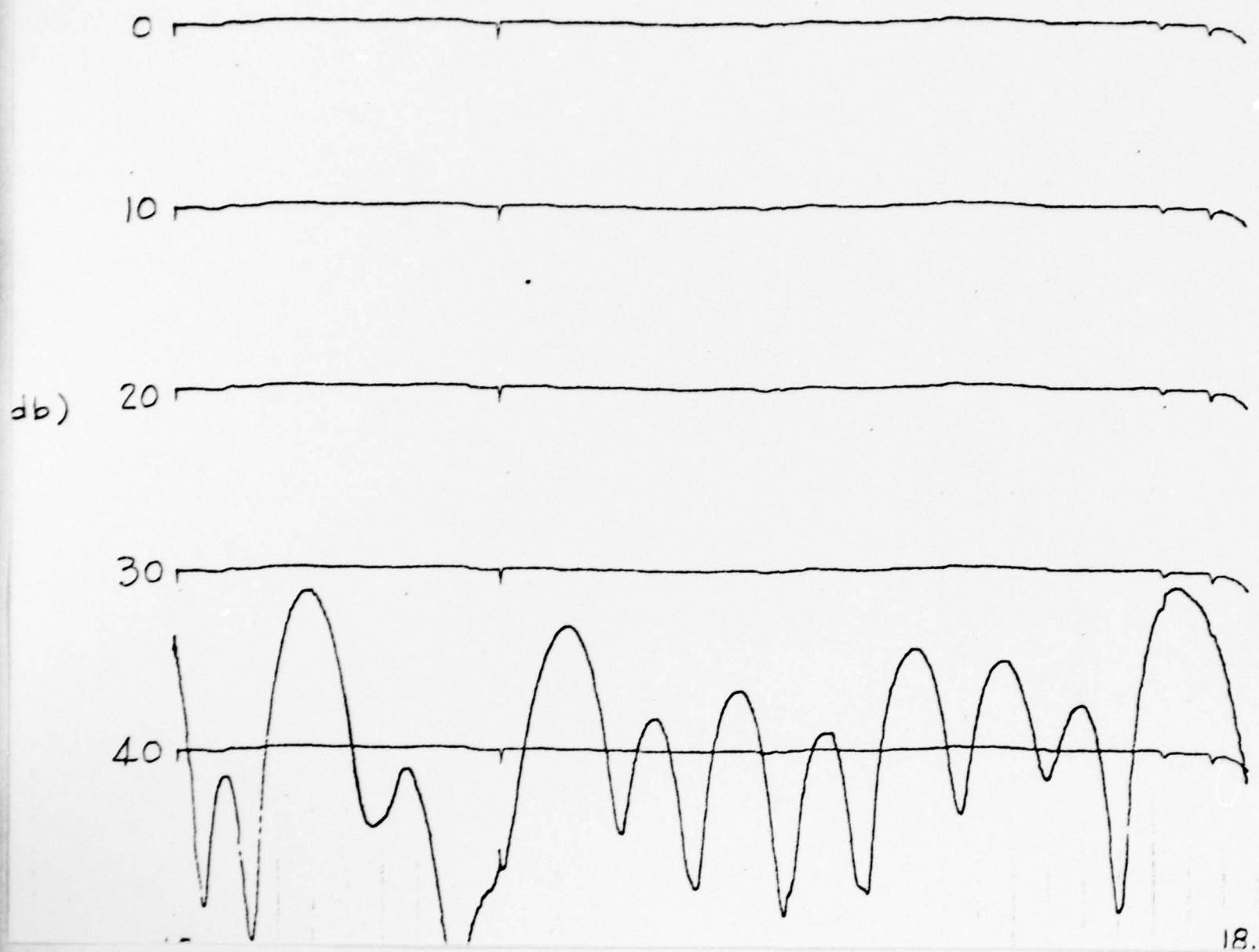

6-18-77

ISOLATION

COLINEAR ARM TO COLINEAR ARM

S/N 5-6

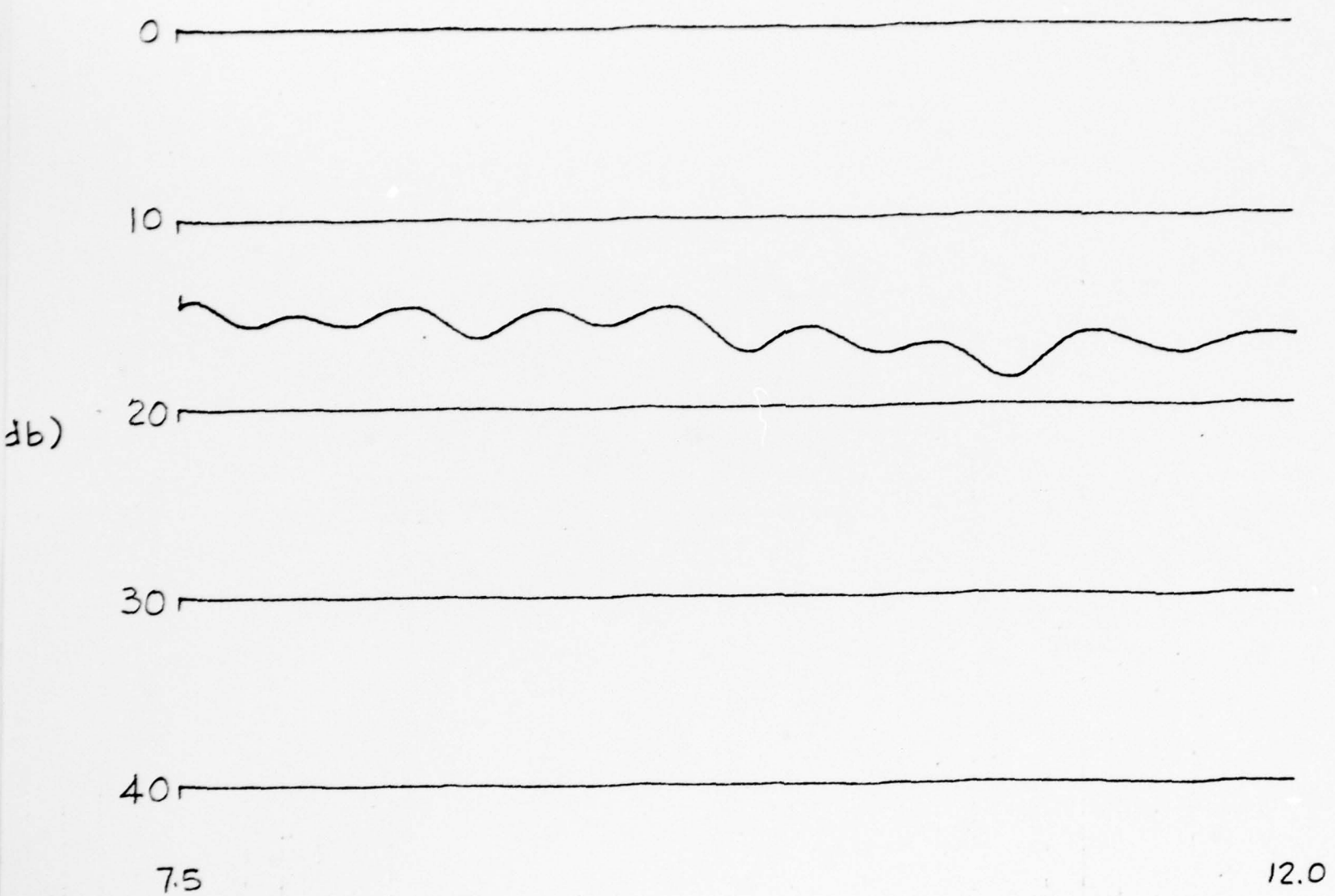

6·18·77

ISOLATION

COLINEAR ARM TO COLINEAR ARM

S/N 5-6

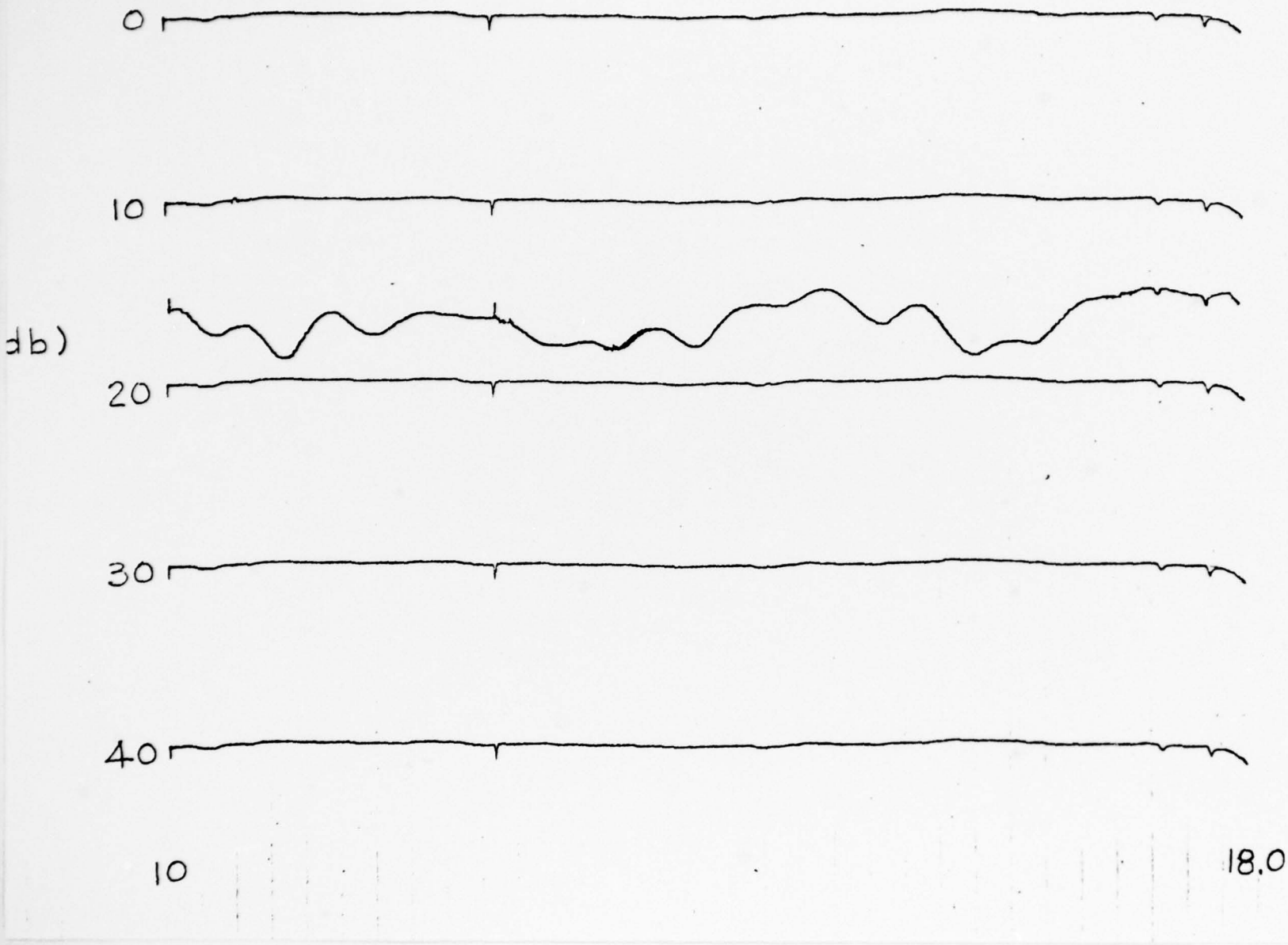

6-18-77

POWER SPLIT

S/N 5-6

△ PORT TO COLINEAR ARMS

RED REF #5
GREEN #6

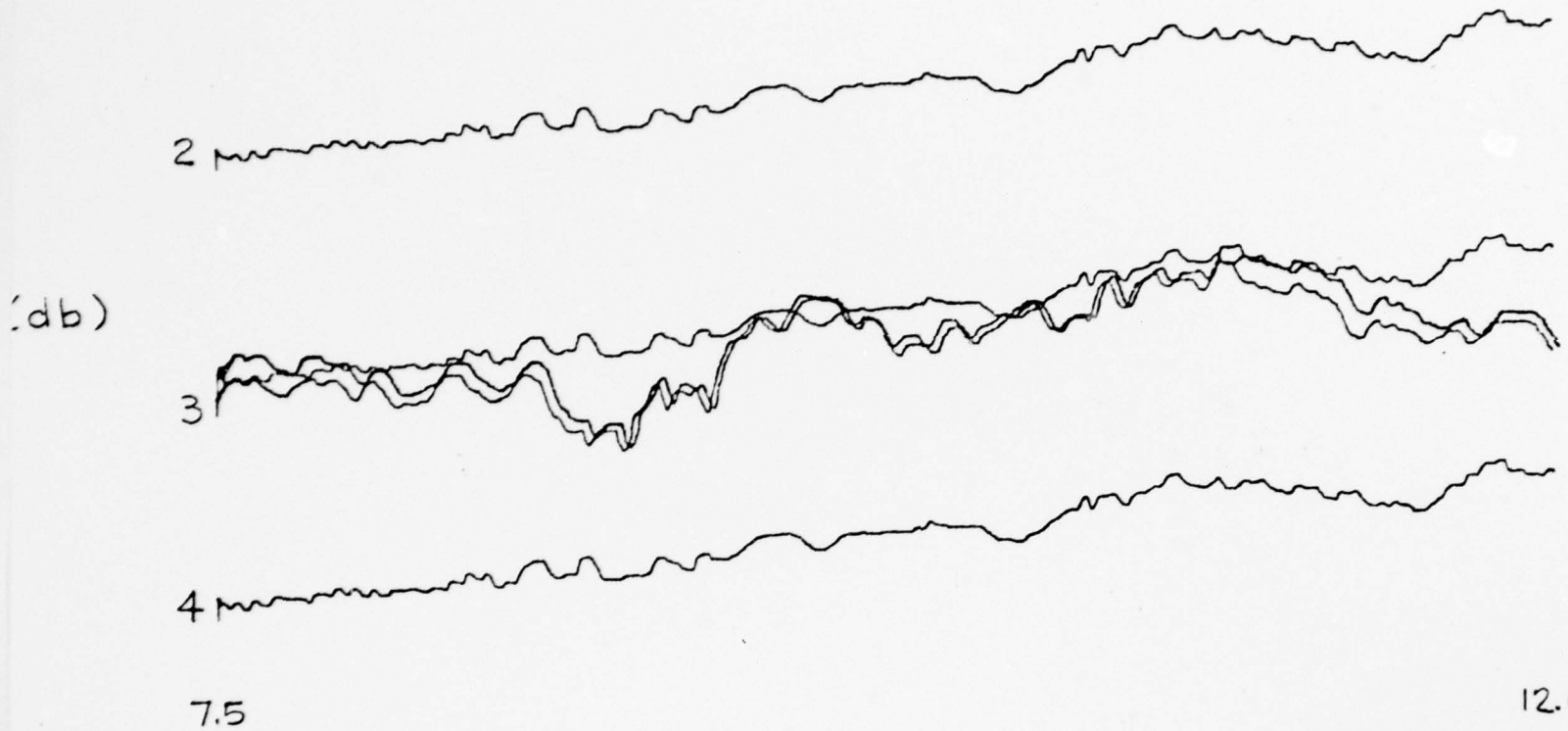

6-18-77

POWER SPLIT

S/N 5-6

△ PORT TO COLINEAR ARMS RED REF #5 GREEN #6

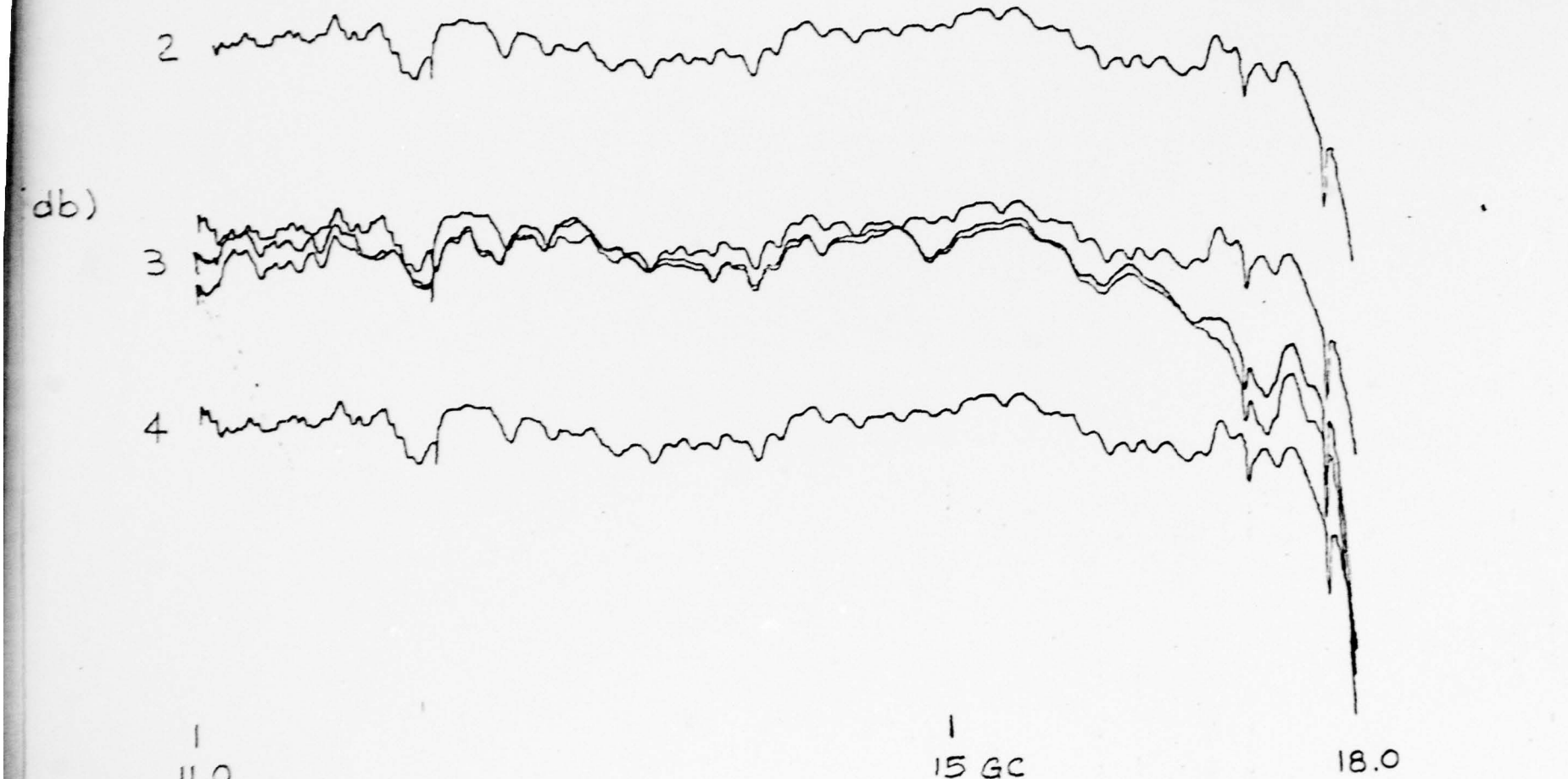

6-18-77

POWER SPLIT

S/N 5-6

△ PORT TO COLINER ARMS RED REF #5
GREEN #6

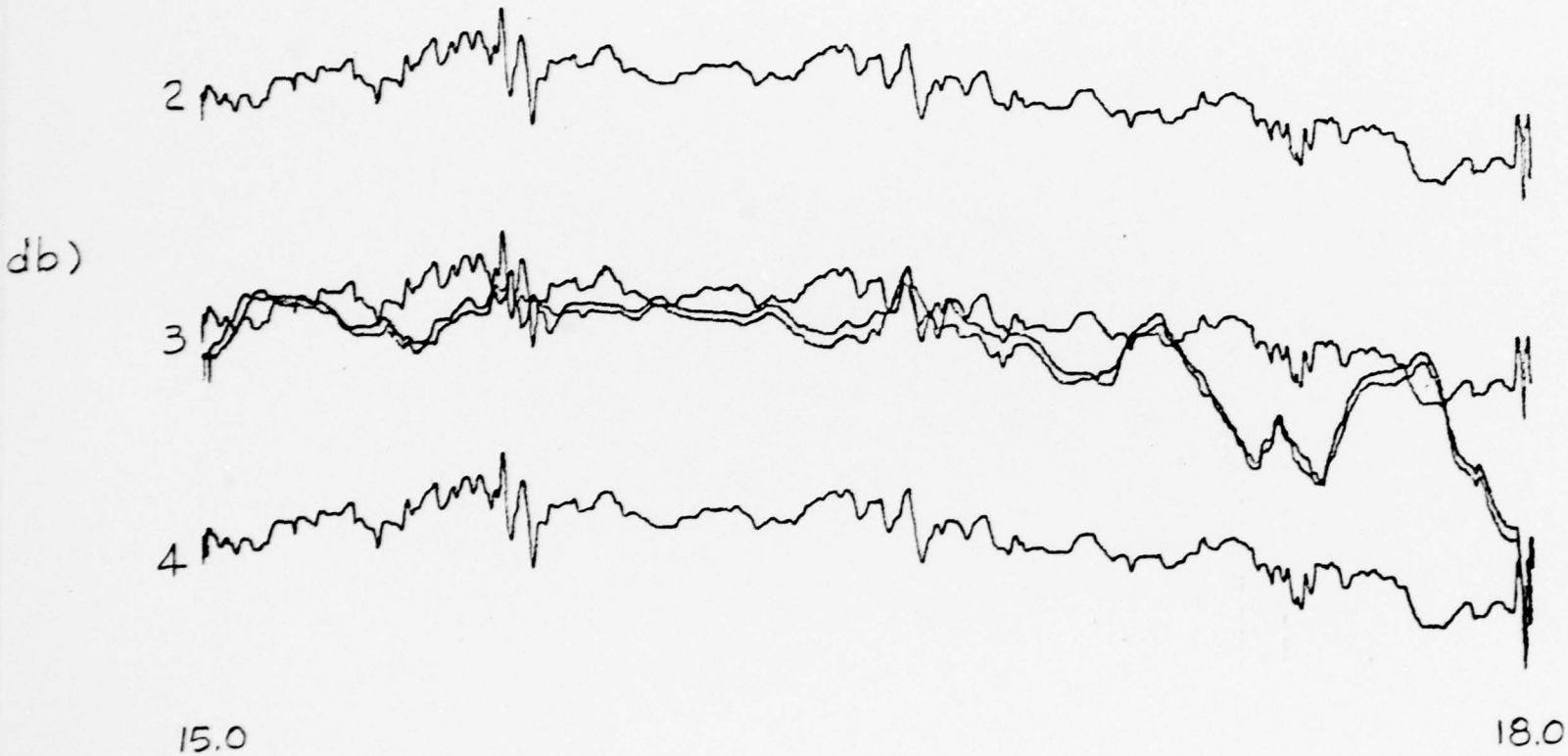

6-18-77

S/N 5-6

POWER SPLIT

Σ PORT TO COLINEAR ARMS

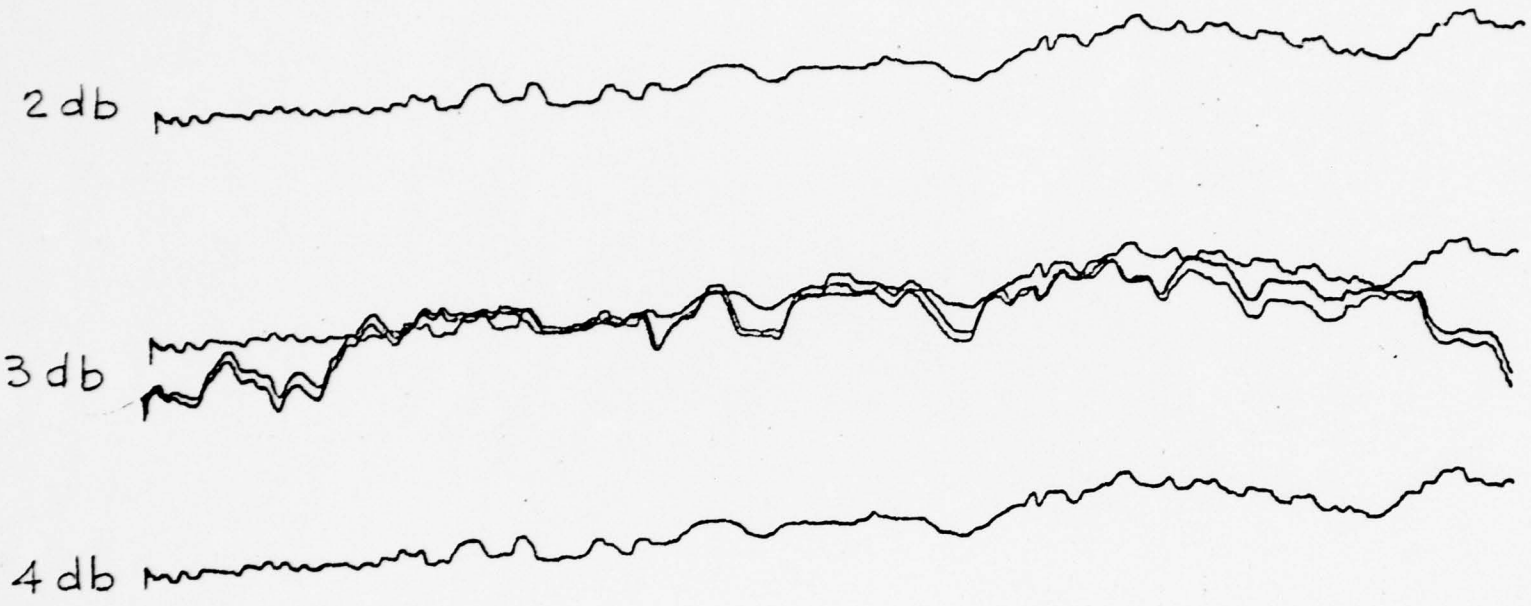

6·18·77

POWER SPLIT

S/N 5-6

Σ PORT TO COLINEAR ARMS

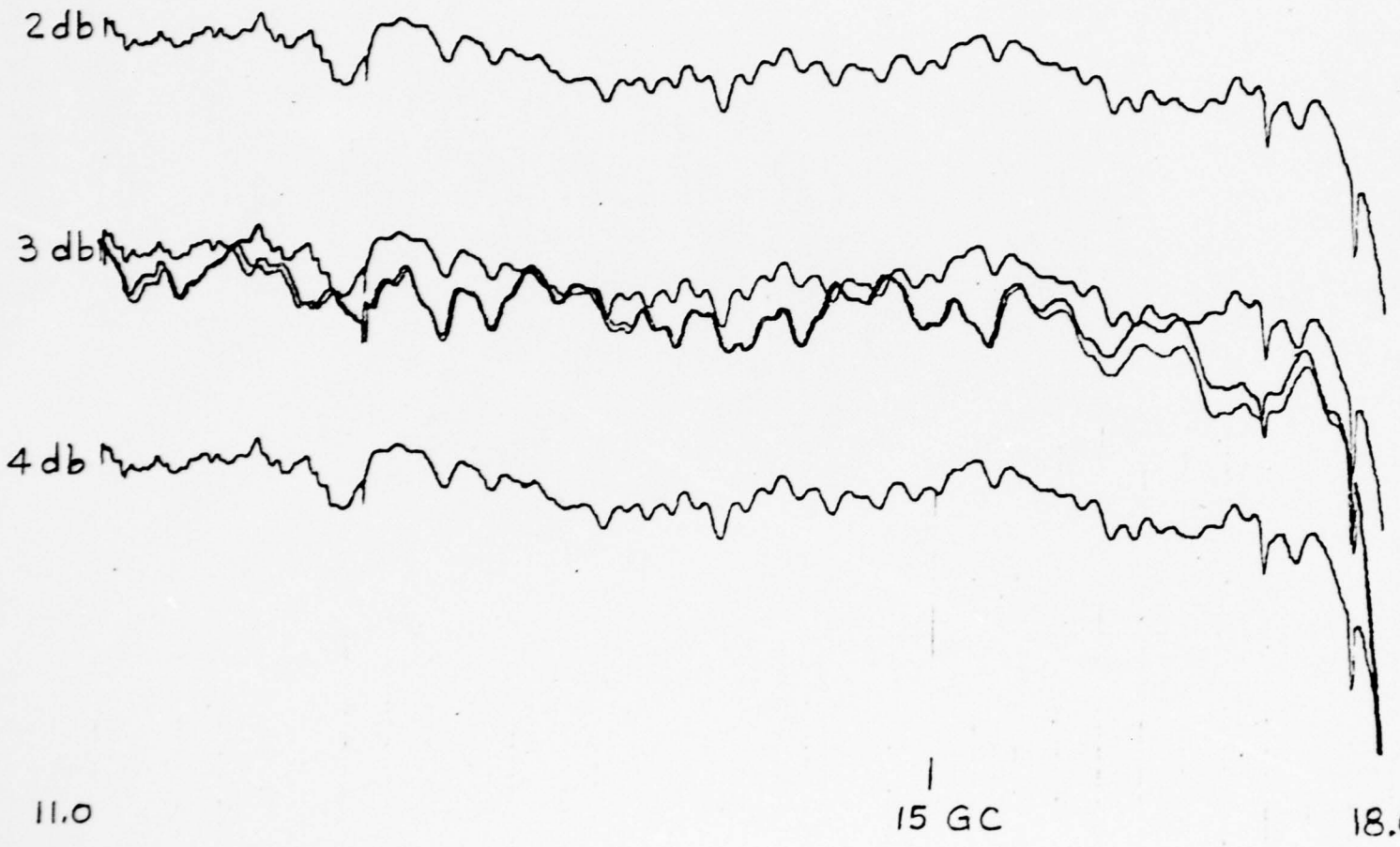

6·18·77

S/N 5-6

POWER SPLIT

Σ PORT TO COLINEAR ARMS

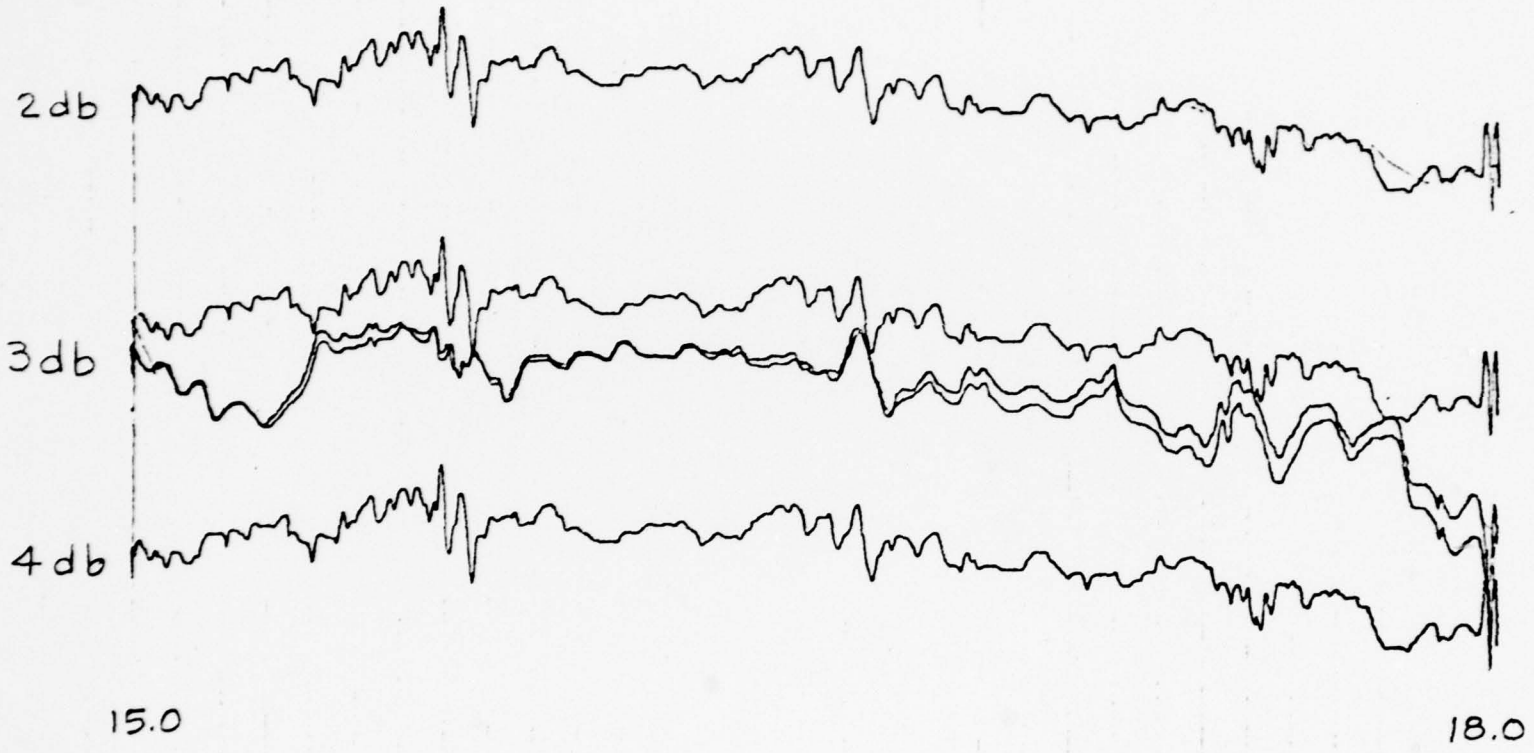

APPENDIX B

COMPUTER PROGRAM FOR HP 9825A

APPENDIX B

COMPUTER PROGRAM FOR HP 9825A

```
0: dsp "MAGIC TEE NETWORK ANALYSIS----10/14/76****    J.W"
1: dim A$[10,18],S$[100,18],E[300],D[300]
2: ent "# OF FREQ.STEPS",M
3: ent " FREQ.INCREMENT",S
4: ent "START FREQ.",G;cfg ;sfg 5
5: prt "     Z     L    Fc "
6: fxd 0;for N=0 to 6
7: if flg5;gto +3
8: cfg 4;if N=0;cfg 4
9: if flg1 or flg4;gto +4
10: str(abs(N))→A$[N+1,1,2]
11: fxd 0;dsp "ELEMENT IMPEDANCE,",N
12: fxd 3;ent "",rN;str(rN)→A$[N+1,3,8]
13: if flg2 or flg4;gto +3
14: fxd 0;dsp "ELEMENT LENGTH,",N
15: fxd 3;ent "",r(N+7);str(r(N+7))→A$[ +1,9,14]
16: if flg3 or flg4;gto +3
17: fxd 0;dsp "ELEMENT CUT-OFF FREQ.,",N
18: fxd 3;ent "",r(N+14);str(r(N+14))→A$[N+1,15,19]
19: cfg 4;prt A$[N+1,3,19]
20: next N
21: for N=21 to 50
22: 0→rN
23: next N
24: cfg
25: for L=0 to M
26: G+LS→F;str(F)→S$[L+1,1,5];11.8/F→W
27: for N=0 to 6
28: W/√(1-(r(N+14)/F)^2)→r(N+41)
29: tan(360*r(N+7)/r(N+41))→r(N+21)
30: rN*r(N+41)/W→r(N+34)
31: next N
32: cfg ;cll 'X COMPLEX'(0,-r37/(r40*r24),0,r27,r30,r31)
33: cll '+ COMPLEX'(1,0,r30,r31,A,B)
34: cll '+ COMPLEX'(0,-r37/(r40*r24),0,r27,C,D)
35: cll '/ COMPLEX'(A,B,C,D,r30,r31)
36: cll '/ COMPLEX'(r10/r30,0,r30,r31,A,B)
37: cll 'X COMPLEX'(r34/(2*r30),0,0,r26,r30,r31)
38: cll '+ COMPLEX'(1,0,r30,r31,r32,r33)
39: cll '+ COMPLEX'(r34/(2*r30),0,0,r26,C,D)
```

```
41: cll '/ COMPLEX'(r30/r36,0,r30,r31,C,D)
42: cll '+ COMPLEX'(A,B,C,D,r30,r31)
43: cll 'I COMPLEX'(r30,r31,A,B)
44: cll '+ COMPLEX'(A,B,0,-(r36/r30r25),A,B)
45: cll 'I COMPLEX'(A,B,C,D)
46: cll 'X COMPLEX'(C,D,0,r23,r30,r31)
47: cll '+ COMPLEX'(1,0,r30,r31,r30,r31)
48: cll '+ COMPLEX'(C,D,0,r23,r32,r33)
49: cll '/ COMPLEX'(r30,r31,r32,r33,A,B)
50: cll 'I COMPLEX'(r35*A/r36,r35*B/r36,C,D)
51: cll 'X COMPLEX'(C,D,0,r22,r30,r31)
52: cll '+ COMPLEX'(1,0,r30,r31,r30,r31)
53: cll '+ COMPLEX'(C,D,0,r22,r32,r33)
54: cll '/ COMPLEX'(r30,r31,r32,r33,A,B)
55: r34*A/r35→A;r34*B/r35→B
56: cll '+ COMPLEX'(1,0,-A,-B,r30,r31)
57: cll '+ COMPLEX'(1,0,A,B,r32,r33)
58: cll '/ COMPLEX'(r30,r31,r32,r33,A,B)
59: 3A→D[L+1];3B→D[L+1]
60: √(A^2+B^2)→X;str(X)→S$[L+1,6,11]
61: str(B/A)→Y;Y*.126/90→Y
62: if sgn(A)<0 and sgn(B)>0;sfg 1
63: if sgn(A)<0 and sgn(B)<0;sfg 2
64: if flg1;Y+.25→Y;gto +2
65: if flg2;Y-.25→Y
66: str(Y)→S$[L+1,12,18]
67: next L
68: prt "*****************"
69: cfg
70: ent "ELEMENT  NEED MOD.",U;val(A$[1,2,6])→r0
71: ent "IMPEDANCE CHANGE?, 0 FOR NO",T;if T=0;sfg 1
72: ent "LENGTH CHANGE?,0 FOR NO",T;if T=0;sfg 2
73: ent "CUT-OFF FREQ. CHANGE? ,0 FOR NO",T;if T=0;sfg 3
74: gto 5;if flg1 and flg2 and flg3;gto 87
75: "+ COMPLEX":
76: p1+p3→p5;p2+p4→p6;ret
77: "X COMPLEX":
78: p1p3-p2p4→p5;p2p3+p1p4→p6;ret
79: "/ COMPLEX":
80: (p1p3+p2p4)/(p3^2+p4^2)→p5
81: (p2p3-p1p4)/(p3^2+p4^2)→p6
82: ret
83: "I COMPLEX":
84: p1/(p1^2+p2^2)→p3
85: -p2/(p1^2+p2^2)→p4
```

```
88: cll 'form'(13.2,11,11)
89: fmt 1,50x,"MAGIC TEE NETWORK ANALYSIS              DATE",/;wrt 6.1
90: fmt 6,43x,"xxxxxxxxxxxxxxxxxxxxxxxxxxxxxxxxxxxxxxxxx",/;wrt 6.6
91: cll 'skip'(5);fmt 2,5x," #      Z        L       Fc  ";wrt 6.2
92: fmt 3,f7.0,1x,f7.3,1x,f7.3,f7.3
93: for I=1 to 7
94: wrt 6.3,val(A$[I,1,2]),val(A$[I,3,8]),val(A$[I,9,14]),val(A$[I,15,18])
95: next I
96: cll 'skip'(2);fmt 4,"        F        AMP        PHI    ";wrt 6.4
97: fmt 5,5x,f5.2,3x,f6.3,5x,f6.3
98: for I=1 to M+1
99: wrt 6.5,val(S$[I,1,5]),val(S$[I,6,11]),val(S$[I,12,18])
100: next I
101: cll 'move'(7,7)
102: cll 'psiz'(6,6,3,6)
103: cll 'scl'(-3,3,-3,3)
104: cll 'xaxis'(0,.5,-3,3)
105: cll 'yaxis'(0,.5,-3,3)
106: for I=1 to M+1
107: cll 'plt'(D[I],D[I],43)
108: next I
109: for N=1 to 3 by 2
110: 0→r49;1→r50;if N=1;3→r50
111: cll 'plt'(Nsin(r49),Ncos(r49),46)
112: if (r49+r50→r49)<=360;gto -1
113: next N
114: wtb 6,12;wtb 6,13
115: ent "ANY MORE MOD.?,0 FOR NO",T;gto 69;if T=0;gto +1
116: stp ;end
117: "move":
118: wtb r0,27,65,int((p1-X)U/64),int((p1-X)U),int((p2-Y)V/64),int((p2-Y)V)
119: ret
120: "imove":
121: wtb r0,27,82,int(p1U/64),int(p1U),int(p2V/64),int(p2V)
122: ret
123: "plt":
124: wtb r0,27,65,int((p1-X)U/64),int((p1-X)U),int((p2-Y)V/64),int((p2-Y)V)
125: if p3=0;46→p3
126: if p3=46;wtb r0,27,82,0,0,0,6
127: wtb r0,p3;wtb r0,8
128: if p3=46;wtb r0,27,82,0,0,63,-6
129: ret
130: "fplt":
131: wtb r0,27,97,int((p1-X)U/64),int((p1-X)U),int((p2-Y)V/64),int((p2-Y)V)
```

```
134: wtb r0,p3;wtb r0,8
135: if p3=46;wtb r0,27,82,0,0,63,-6
136: ret
137: "iplt":
138: wtb r0,27,82,int(p1U/64),int(p1U),int(r2V/64),int(p2V)
139: if p3=0;46→p3
140: if p3=46;wtb r0,27,82,0,0,0,6
141: wtb r0,p3;wtb r0,8
142: if p3=46;wtb r0,27,82,0,0,63,-6
143: ret
144: "fiplt":
145: wtb r0,27,114,int(r1U/64),int(p1U),int(r2V/64),int(r2V)
146: if p3=0;46→p3
147: if p3=46;wtb r0,27,82,0,0,0,6
148: wtb r0,p3;wtb r0,8
149: if p3=46;wtb r0,27,82,0,0,63,-6
150: ret
151: "char":
152: if r2=0;5→p2;0→p3
153: wtb r0,27,46,p1,int(p2/64),r2,r3
154: ret
155: "psiz":
156: p1→H;r2→W
157: wtb r0,27,70,int(p4*120/64),p4*120,int(r3*96/64),p3*96
158: ret
159: "scl":
160: 120W/(p2-p1)→U
161: 96H/(p4-p3)→V
162: p1→X;p3→Y
163: ret
164: "xaxis":
165: wtb r0,27,46,95,0,5,9
166: if r3=0 and p4=0;X→p3;X+120W/U→p4
167: if p2=0;p4-p3→p2
168: wtb r0,27,65,int((r3-X)U/64),int((r3-X)U),int((p1-Y)V/64),int((r1-Y)V)
169: p3→p5;wtb r0,43;wtb r0,8
170: wtb r0,27,114,int(p2U/64),int(p2U),0,0;wtb r0,43,8;jmp (p5+p2→p5)>=p4
171: ret
172: "yaxis":
173: wtb r0,27,46,124,0,3,0
174: if r3=0 and p4=0;Y→p3;Y+96H/V→p4
175: if p2=0;p4-p3→p2
176: wtb r0,27,65,int((p1-X)U/64),int((r1-X)U),int((r3-Y)V/64),int((r3-Y)V)
177: p3→p5;wtb r0,43;wtb r0,8
```

```
180: "space":
181: if p1<0;gto +2
182: wtb r0,32;jmp 2((p1-1→p1)=0)
183: wtb r0,8;jmp (p1+1→p1)=0
184: ret
185: "skip":
186: if p1<0;gto +2
187: wtb r0,10;jmp 2((p1-1→p1)=0)
188: wtb r0,27,10;jmp (p1+1→p1)=0
189: ret
190: "copy":
191: if p2=0;6→p2
192: wtb r0,27,86,int(96/p2/64),96/p2
193: if p1<0;wtb r0,27,80;ret
194: wtb r0,27,72,int(120/p1/64),120/p1
195: ret
196: "form":
197: wtb r0,27,77
198: wtb r0,27,84
199: if p1=0;13.2→p1;11→p2→p3
200: wtb r0,27,87,int(120*p1/64),120*p1
201: wtb r0,27,76,int(96*p2/64),96*p2
202: wtb r0,27,70,int(96*p3/64),96*p3
203: ret
204: "ptyp":
205: rdb(0)→I;if I=1;ret
206: if I<124;gto +12
207: if I>224 and I<251;I-160→I;gto +15
208: if I>176 and I<182;I-144→I;gto +14
209: if I=182;38→I;gto +13
210: if I=183;64→I;gto +12
211: if I=184;91→I;gto +11
212: if I=185;93→I;gto +10
213: if I=222;92→I;gto +9
214: if I=251;124→I;gto +8
215: if I=191;58→I;gto +7
216: if I=176;39→I;gto +6
217: if I=171 or I=172;I-112→I;gto +5
218: if I>77 and I<88;I-30→I;gto +4
219: if I=88;46→I;gto +3
220: if I=94;wtb r0,14
221: if I=89;44→I
222: wtb r0,I;gto -17
223: "view":
224: wtb r0,27,68,int(p1/64),p1
```